



Bruker Educational SC-XRD Webinar

Smallest Crystals: How Modern Microfocus Sources Can Help You Determine the Structure From Weak Diffractors

The background of the slide is a blue-tinted collage. It features a periodic table of elements with various chemical symbols like Na, Mg, K, Ca, Sc, Ti, Rb, Sr, Y, Zr, Cs, Ba, La, Hf, V, Cr, Mn, Fe, Co, Ni, Cu, Zn, Ga, In, Sn, Pb, Ta, Re, Fr, Ra, Ac, Ce, Pr, Nd, P, Bi, Po, U, Np, Pu, Am, Cm, Bk, Cf, Es, Fm, Md, No, Lr. Overlaid on this are several 3D ball-and-stick molecular models of organic and inorganic compounds. On the right side, there is a blue ribbon diagram representing a protein structure. At the bottom left, there is a diagram of X-ray diffraction with a central point source, a vertical axis, and several concentric semi-circular arcs representing diffraction rings. A dashed arrow points from the source towards the rings.

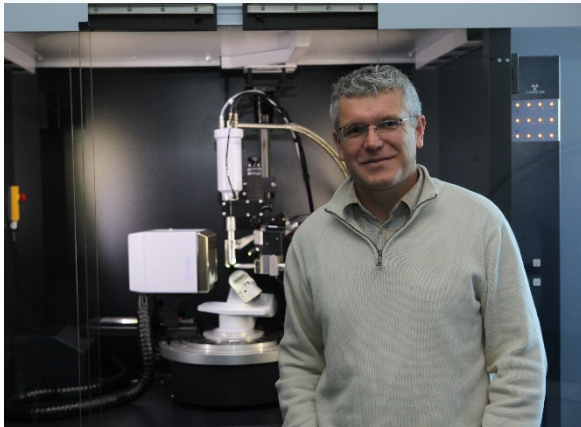
Dr. Michael Ruf
Senior Product Manager
Bruker AXS

Dr. Jürgen Graf
Application Scientist & Product
Manager μ S
Incoatec GmbH

June 19, 2020

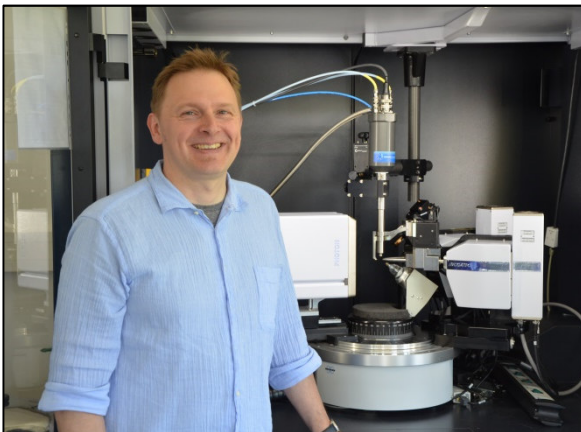
1

Who is talking?



Dr. Michael Ruf:

- In Madison, USA
- Senior Product Manager
- PhD in Chemistry
- Joined Bruker AXS in 1998
- Michael.Ruf@bruker.com



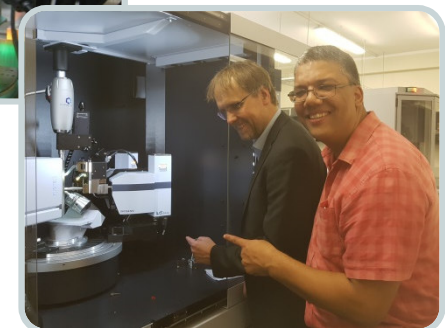
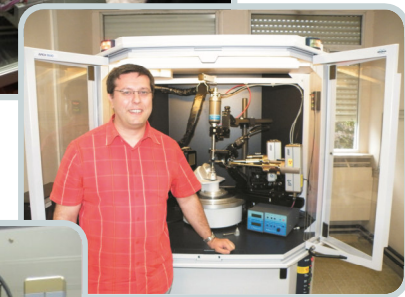
Dr. Juergen Graf:

- In Geesthacht, Germany
- Application Scientist & Product Manager I μ S
- PhD in Chemistry
- Joined Incoatec in 2004
- Juergen.Graf@incoatec.de

The I μ S Success Story

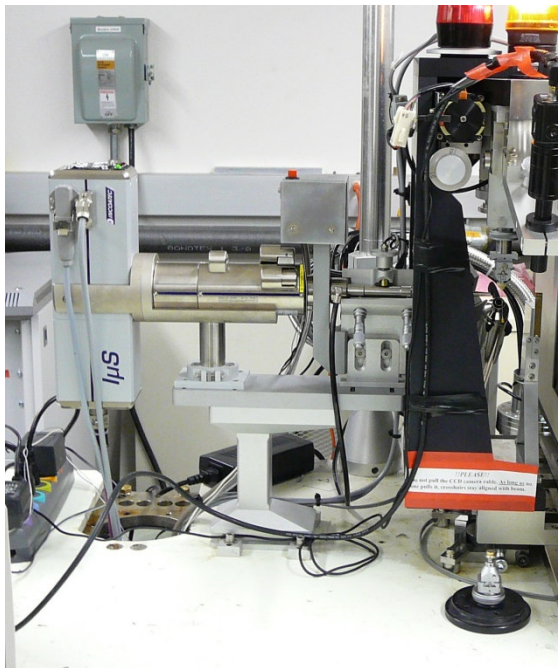


- 2002 Foundation of Incoatec as joint venture with Bruker
- 2006 Cu-I μ S for PX and SAXS
- 2007 1st I μ S is installed at Univ. Kiel
 - Mo-I μ S for Chemical Crystallography
 - Cu-I μ S for XRD²
- 2009 Ag-I μ S for Solid State Chemistry,
High-Pressure and Charge Density Research
- 2010 100th I μ S is installed at CNRS Lille
- 2011 I μ S^{High Brilliance} family with D8 VENTURE
- 2015 500th I μ S Customer at Univ. Göttingen
 - I μ S 3.0** (AsCA Kolkata)
- 2017 **I μ S DIAMOND** (IUCr Hyderabad)
- 2020 1000th I μ S is installed at Univ. Cape Town

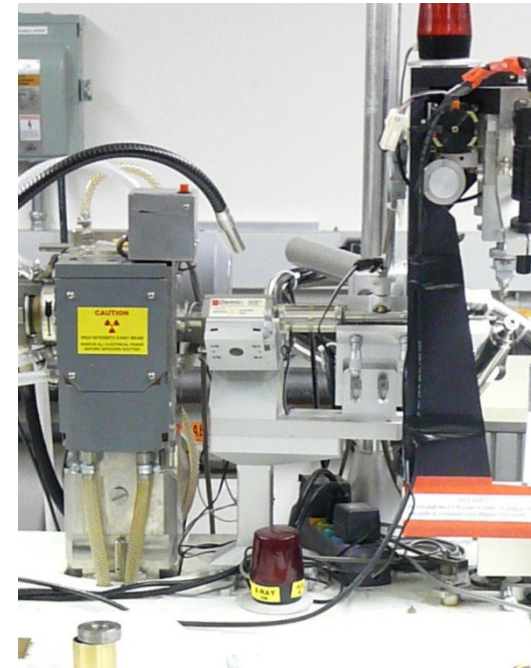


Revolution without Revolutions

- One of the first upgrades: Replacing a 4 kW rotating anode by a 30 W $I\mu S$ used for protein screening



30 W Cu- $I\mu S$ plus IP Detector



4 kW Rotating Anode plus IP Detector

IXT Manufacturing at INCOATEC



The I μ S 3.0: Microfocus Made Perfect

- The I μ S 3.0 is the first and only source **designed** specifically **for crystallography** with no compromises
- I μ S 3.0 features
 - more than **twice the intensity** of competing 30 W microfocus sources!
 - about **50% more intensity** compared competing 50 W HB-class microfocus sources!
- Complete **mechanical redesign** for maximum customer convenience
- No more vacuum pump
- Same extraordinary **reliability**
 - 3-year warranty
 - typical tube lifetime > 5 years
 - still no water cooling required!

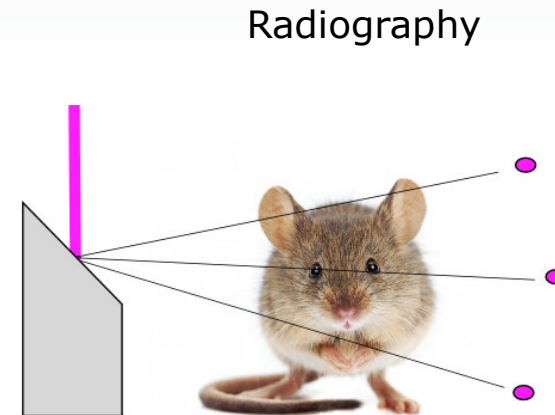


What is Special About a Tube Optimized for Crystallography?



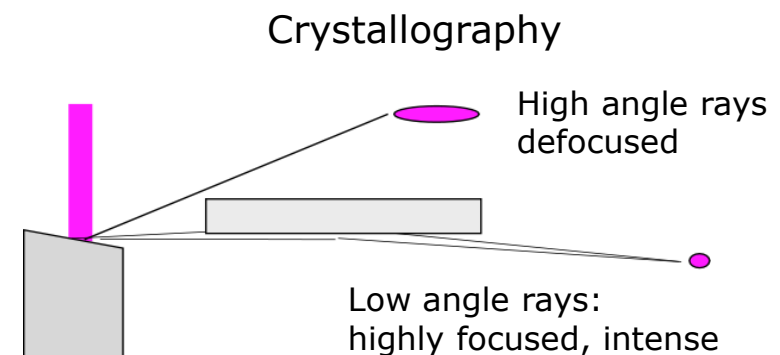
- All other microfocus tubes on the market were designed primarily for radiography (medical or NDT)

They therefore feature high take-off angles in order to preserve resolution over a wide field of view



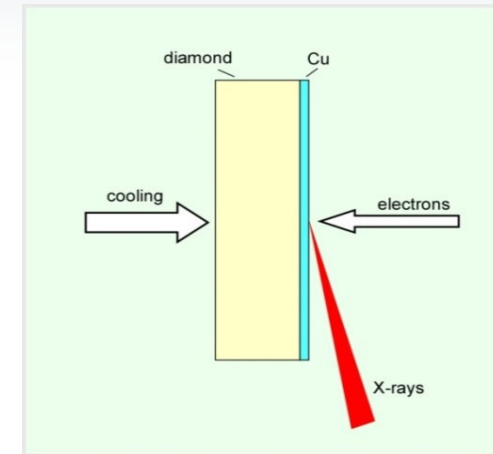
- In crystallography we do not need a wide field of view, we only need to produce an intense beam of X-rays

An elongated electron beam focus on an anode with a lower take-off angle produces higher intensity



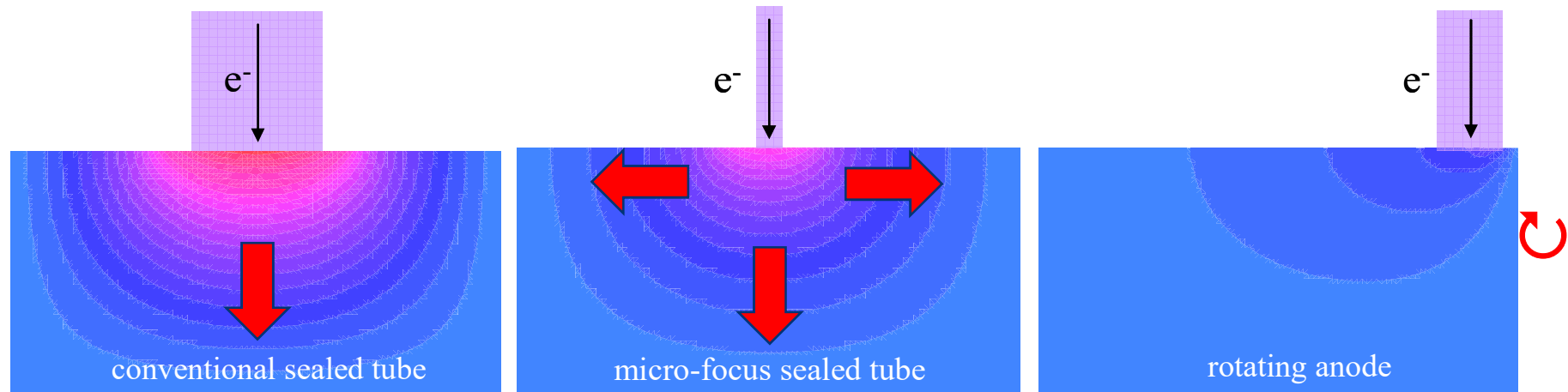
What is the I μ S DIAMOND?

- The first microfocus tube that uses an advanced **Diamond Hybrid Anode**
 - Diamond heat sink improves heat dissipation
 - Increased power density on anode
- Coupled to **synchrotron-class** multilayer Montel optics
- Intensity of modern microfocus rotating anodes
 - **Twice the intensity** of competing 50 W HB-class sources
- Same proven mechanical platform and same lifetime as I μ S 3.0
- No routine maintenance
- Available for Cu, Mo and Ag radiation



Brightness of Microfocus Sources

- Power Load in All Solid-target X-ray Sources is Limited by Heat Dissipation



- Large Spot
- Quasi-1D heat flow limits power density
- $\sim 0.5 \text{ kW/mm}^2$

- Small Spot
- 2D heat flow allows more efficient cooling
- $\sim 5 \text{ kW/mm}^2$

- Large or Small Spot
- Additional heat spread by rotation
- $> 15 \text{ kW/mm}^2$

Relative B: 1

Relative B: ~ 10

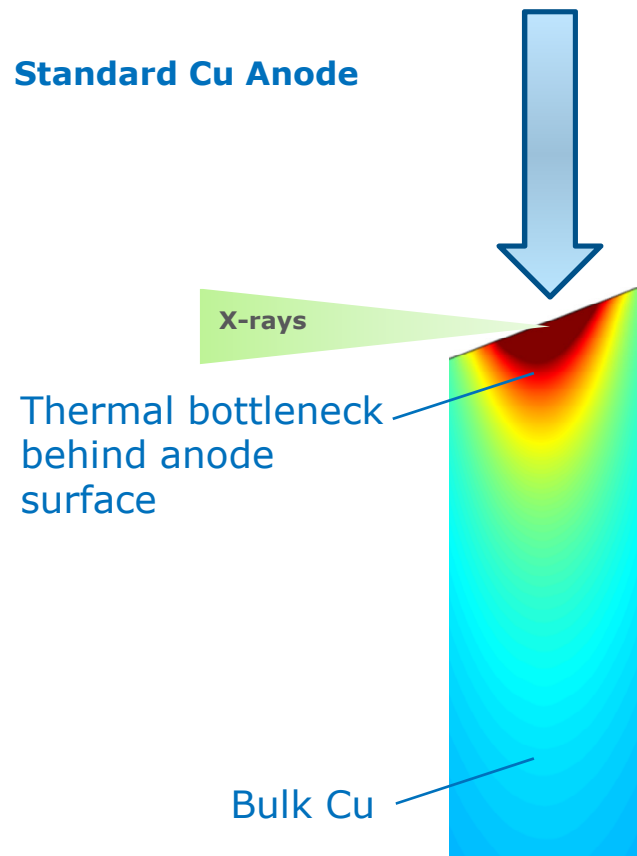
Relative B: > 10

What is the I μ S DIAMOND?

I μ S 3.0

Standard Cu Anode

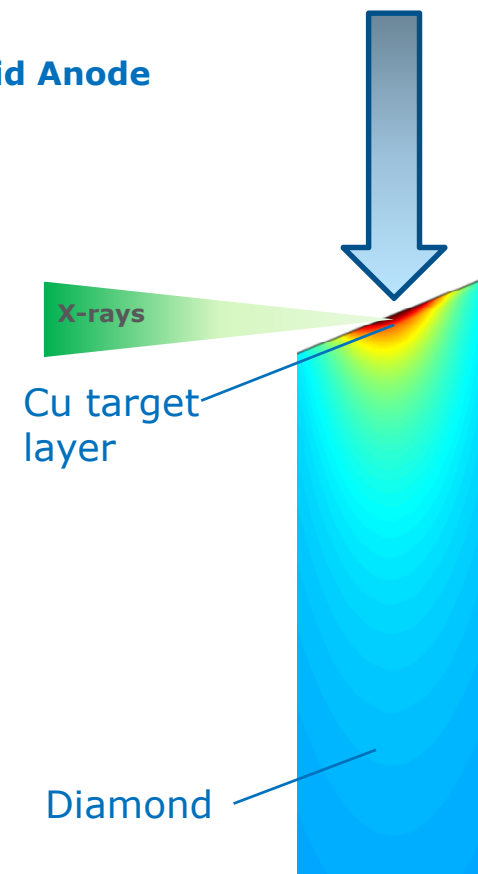
E-beam



I μ S DIAMOND

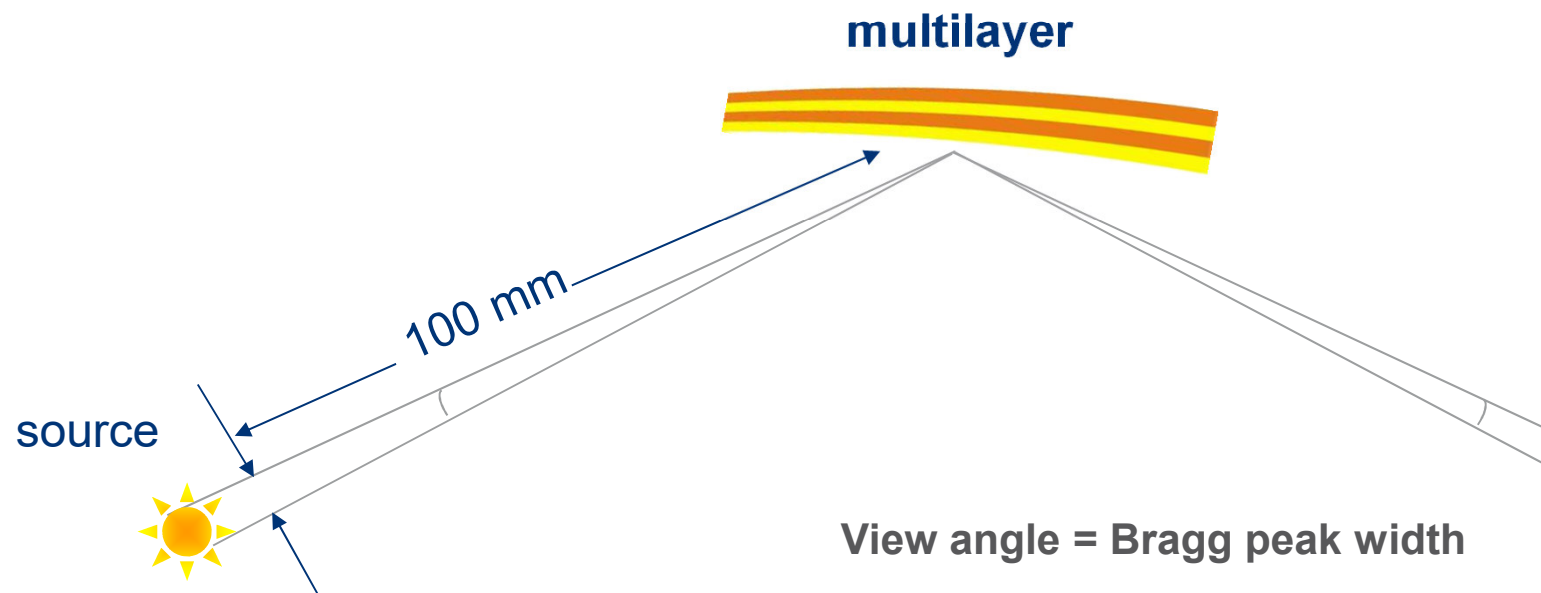
Diamond Hybrid Anode

E-beam



The Perfect Match

- Multilayer Mirrors and Microfocus Sources are a **Perfect Match** for monochromatic beam with tailored beam cross-section and divergence
- **View angle** of the multilayer coating **fits the source size**



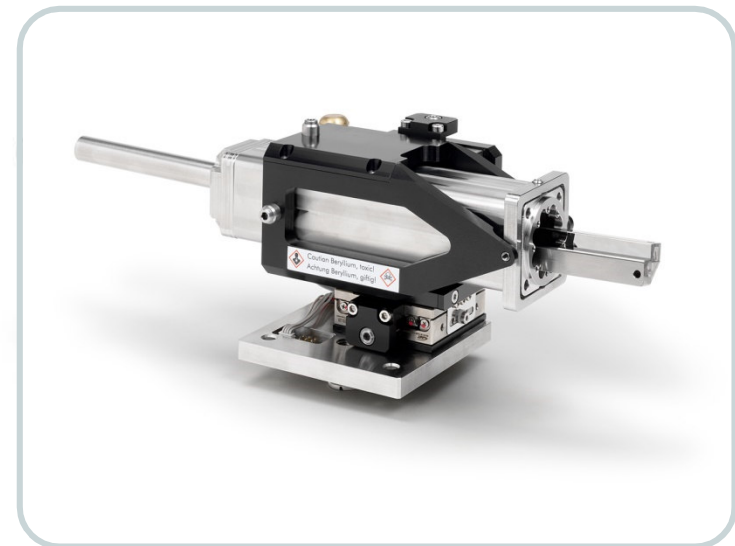
$$100 \text{ mm} * 1 \text{ mrad} = 100 \text{ } \mu\text{m}$$

View angle = Bragg peak width

Typical for W/C multilayer:
FWHM = 1 mrad for Cu K α (= 0.057°)

HELIOS EF Optics

- HELIOS EF optics is **designed** for the **Cu-I μ S 3.0** to deliver a high intensity in a sharply focused beam
- **Large divergence** that matches the typical mosaicity of small and weakly diffracting samples in **chemical crystallography**
- **Twice the intensity** of the HELIOS MX optics

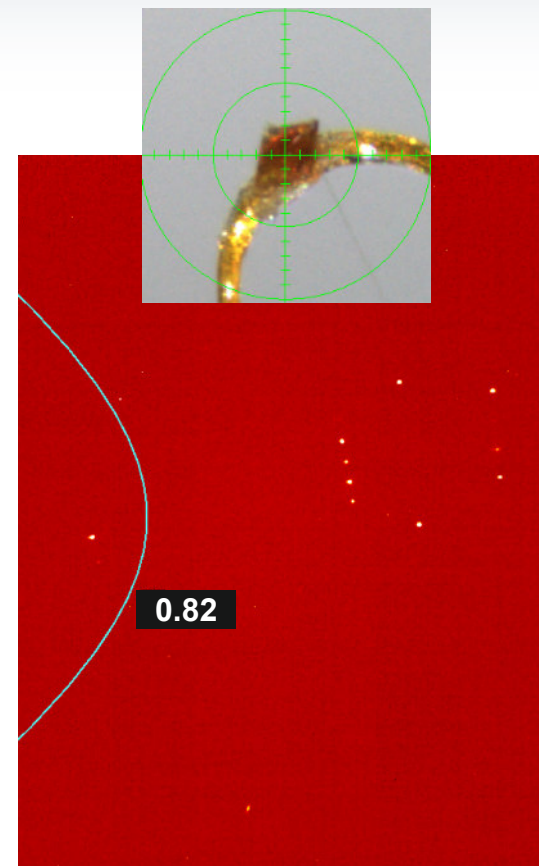


	HELIOS MX	HELIOS EF
Divergence [mrad]	7.5	13.5
FWHM [mm]	0.10	0.10
Intensity [phts/s/mm ²]	> 3.5 10 ¹⁰	> 7.7 10 ¹⁰

HELIOS EF Optics

- Data Comparison for Small Vitamin C Crystal

Size [mm ³]	0.04 x 0.10 x 0.10	
Optics	HELIOS MX	HELIOS EF
Exposure time [s/°]	4 / 8	4 / 8
Ratio of norm. $\langle I \rangle$	1	2.14
$\langle I/\sigma \rangle$	27.1 (11.2)	37.0 (25.1)
$R(\text{int})$ [%]	4.91 (14.66)	3.75 (6.82)
$R1, wR2$ [%]	3.27; 7.51	2.59; 6.65
Parsons $z(v)$	0.16(13)	0.02(8)
$d(\text{C-C})$ [Å]	1.526(5)	1.527(3)

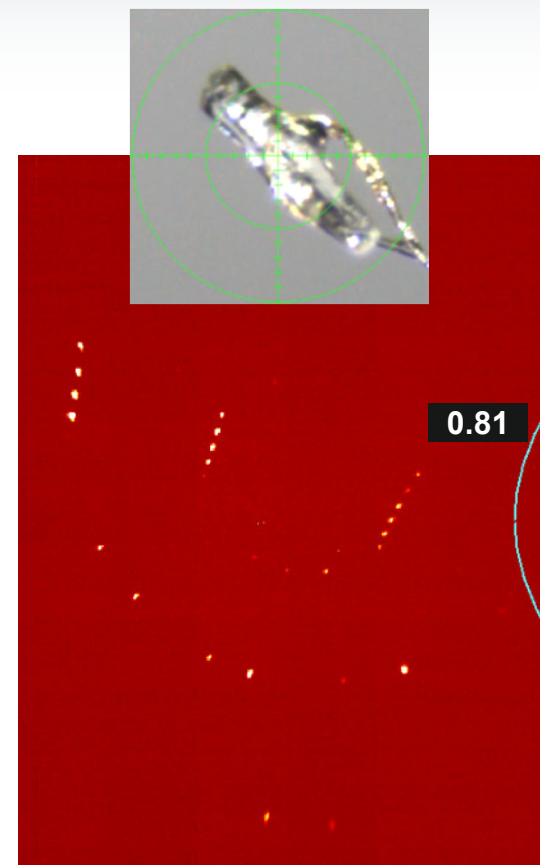
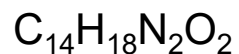


Typical diffraction pattern ($P2_1$,
 $a = 6.3962(2)$ Å, $b = 6.3166(2)$ Å,
 $c = 17.0992(5)$ Å, $\beta = 99.347(2)^\circ$, $Z = 4$)

HELIOS EF Optics

- Real Life Example: Larger Crystal of Amide Derivative

Size [mm ³]	0.05 x 0.10 x 0.35	
Optics	HELIOS MX	HELIOS EF
Exposure time [s/°]	6 – 12	6 – 12
Resolution [Å]	0.81 (0.91 – 0.81)	0.81 (0.91 – 0.81)
Multiplicity	9.7 (5.2)	9.6 (7.2)
$\langle I/\sigma \rangle$	54.0 (32.2)	69.9 (55.3)
$R1, wR2$ [%]	2.75; 6.84	2.65; 7.05
Parsons $z(v)$	0.04(5)	0.01(4)
$d(C-C)$ [Å]	1.525(3) 1.384(3)	1.527(2) 1.385(2)



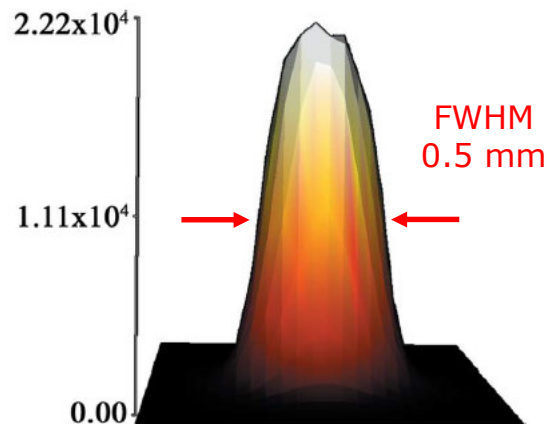
Typical diffraction pattern ($P2_12_12_1$,
 $a = 6.0471(2)$ Å, $b = 9.2264(3)$ Å,
 $c = 23.0208(8)$ Å, $Z = 4$)

Beam Profile

Top Hat vs. Gaussian Beam Profile

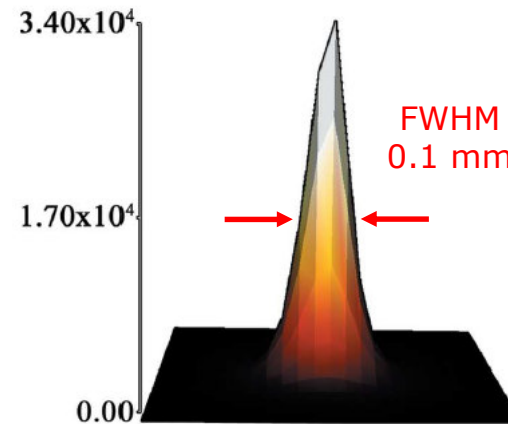
Comparison of beam profiles from a focusing multilayer X-ray mirror and from a flat graphite monochromator

Flat Graphite Monochromator



Top-hat beam profile
FWHM depends on collimator
Constant flux density

Multilayer Mirror

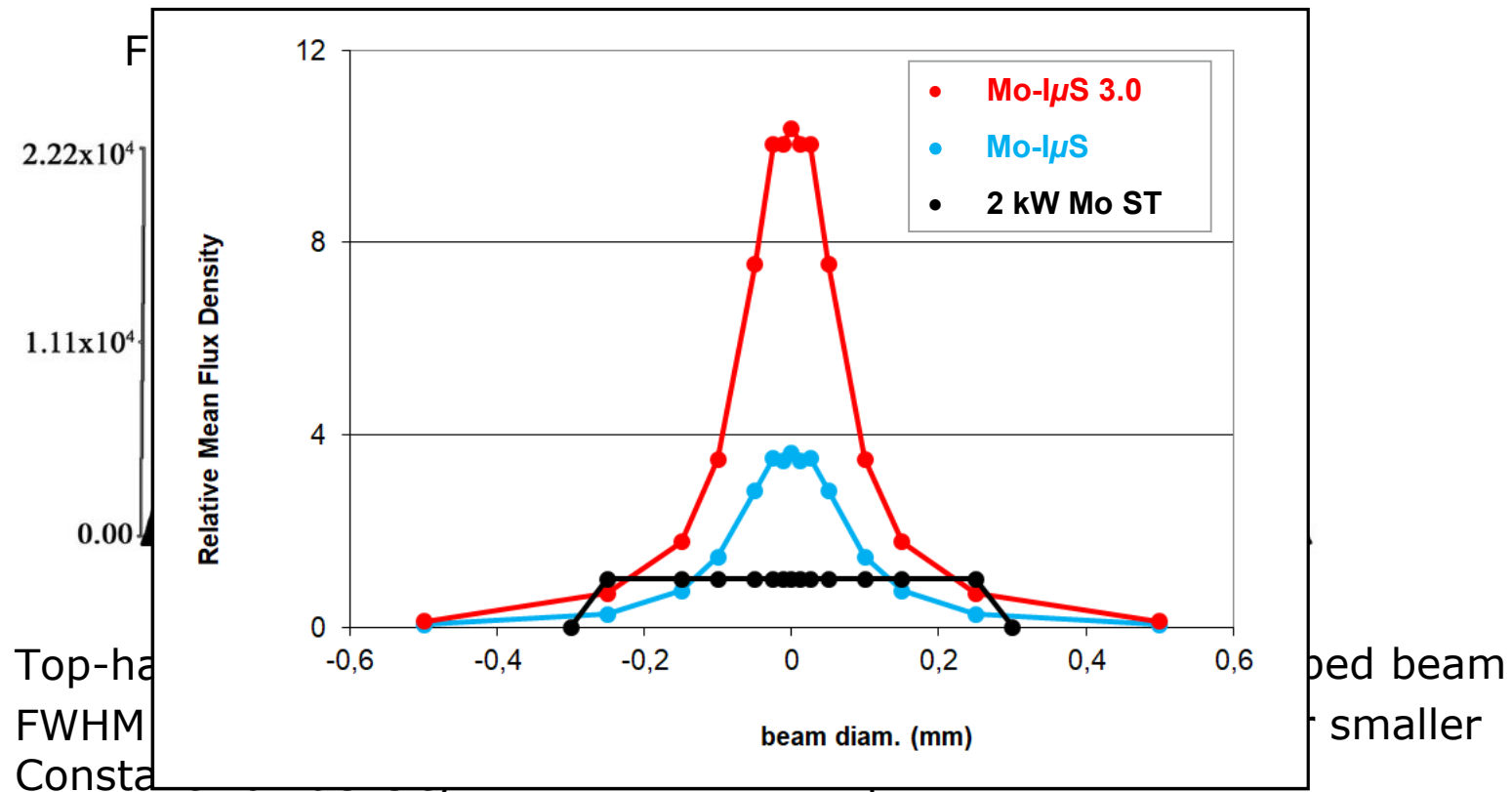


- Symmetric Gaussian shaped beam
- Flux density increases for smaller sample diameters

Beam Profile

Top Hat vs. Gaussian Beam Profile

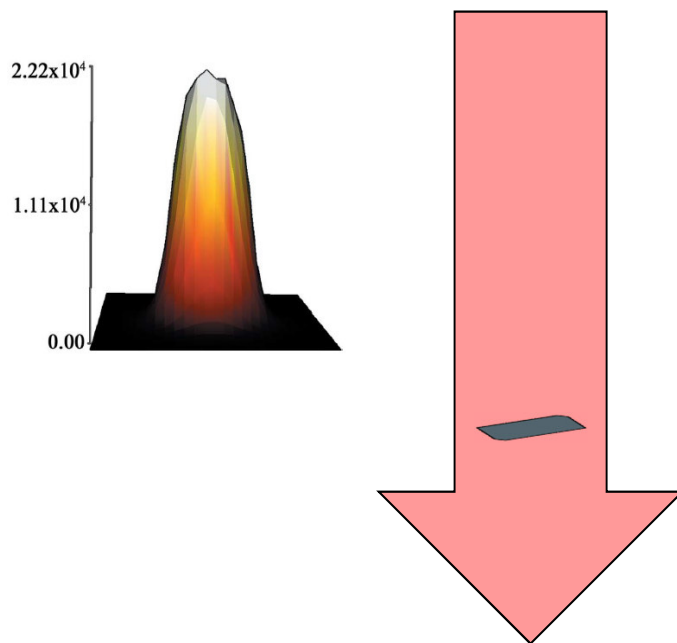
Comparison of beam profiles from a focusing multilayer X-ray mirror and from a flat graphite monochromator



Beam Profile

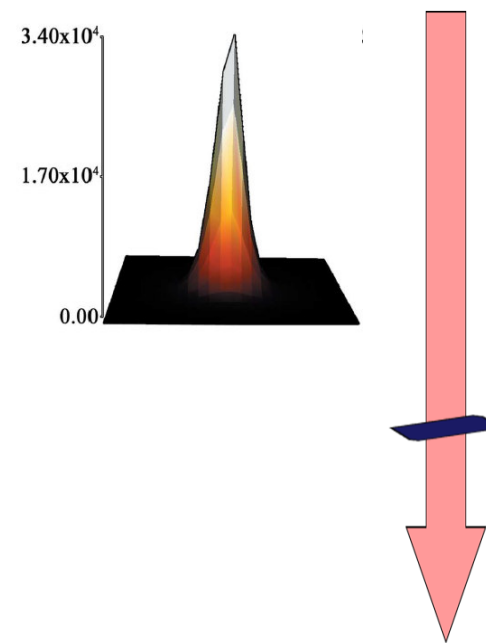
Top Hat vs. Gaussian Beam Profile

Top hat beam



Crystal bathed in beam of uniform intensity. Effective diffracting volume does not change on rotating.

Focusing optics

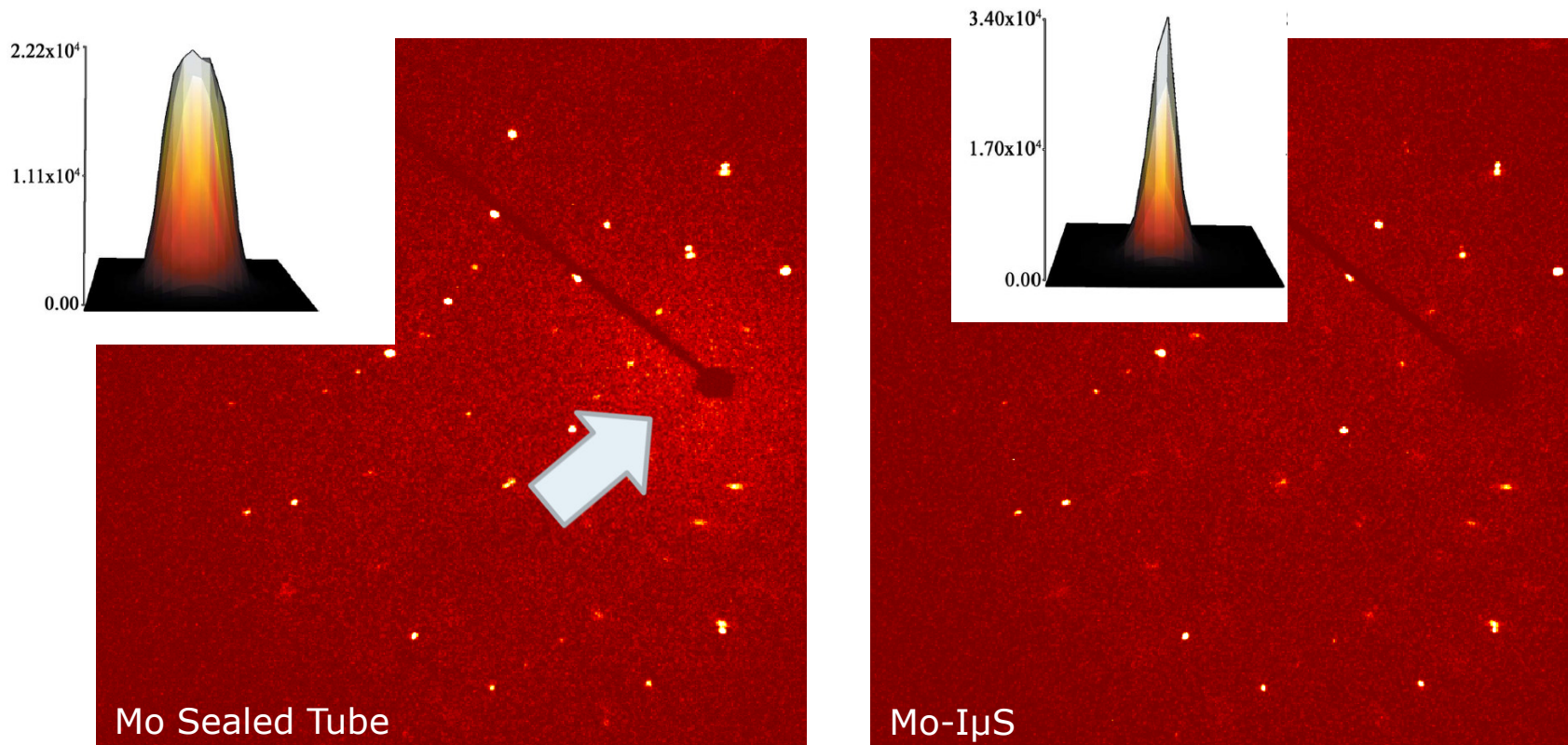


Effective diffracting volume might vary with crystal orientation. Scaling will correct for this. The standard face-indexed correction is inappropriate.

Beam Profile

Top Hat vs. Gaussian Beam Profile

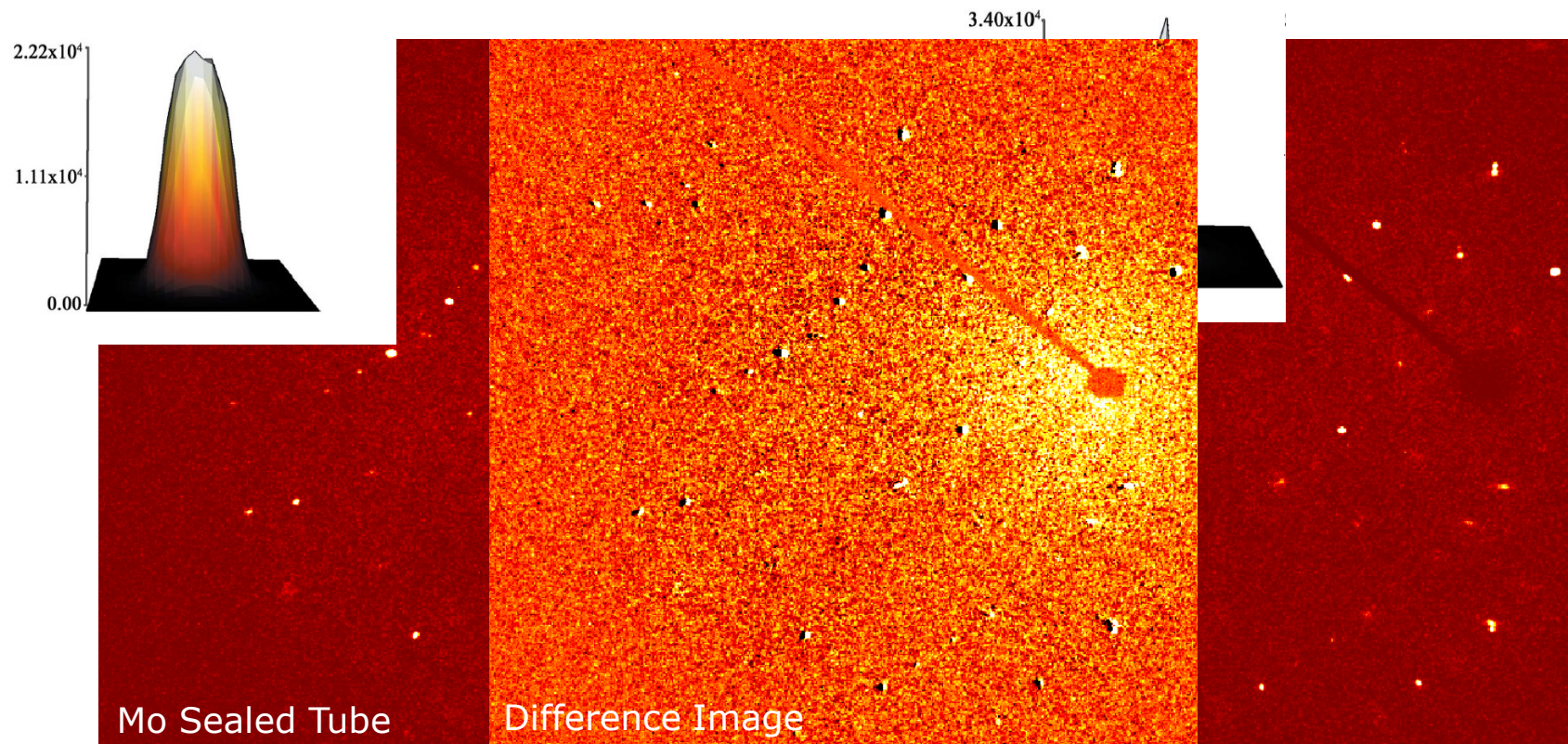
- Top hat beam has more background noise due to more air scattering



Beam Profile

Top Hat vs. Gaussian Beam Profile

- Top hat beam has more background noise due to more air scattering

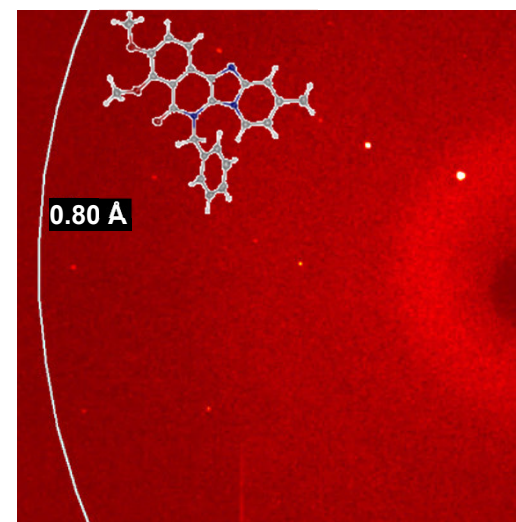
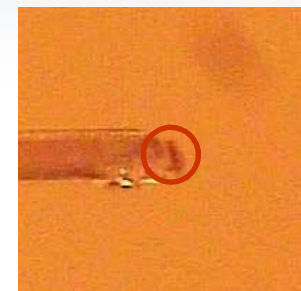


Beam Profile

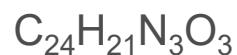
Top Hat vs. Gaussian Beam Profile

- Data comparison from Small Crystal of Organic Compound

Size [mm ³]	0.05 x 0.05 x 0.10	
Source	Mo ST	Mo-I μ S
Power [W]	2000	30
Exposure time	90 s/0.3°	30 s/0.3°
Resolution [Å]	0.75 (0.85 – 0.75)	0.75 (0.85 – 0.75)
Ratio norm. < I >	1	7.3
< I/σ >	10.7 (2.1)	15.3 (3.5)
R1, wR2 [%]	5.55, 10.44	3.88; 9.16
Distance N – C [Å]	1.325(4)	1.325(3)



Typical diffraction pattern ($P2_1$,
 $a = 8.3628(6)$ Å, $b = 7.0469(5)$ Å,
 $c = 15.9737(11)$ Å, $\beta = 92.210(1)^\circ$, $Z = 2$)

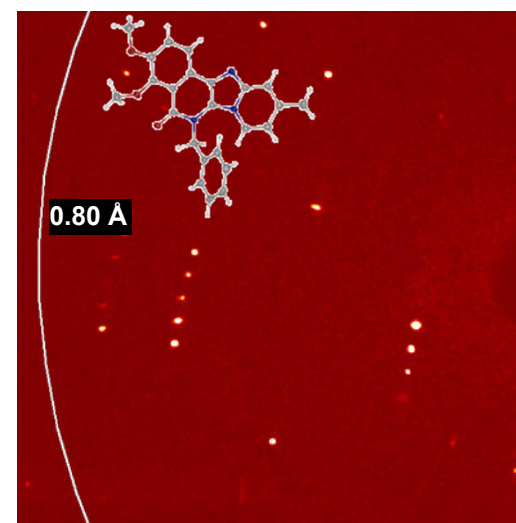


Beam Profile

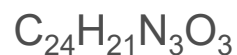
Top Hat vs. Gaussian Beam Profile

- Data comparison from Large Crystal of Organic Compound

Size [mm ³]	0.15 x 0.25 x 0.30	
Source	Mo ST	Mo-I μ S
Power [W]	2000	30
Exposure time	15 s/0.3°	10 s/0.3°
Resolution [Å]	0.75 (0.85 – 0.75)	0.75 (0.85 – 0.75)
Ratio Norm. < I >	1	3.7
< I/σ >	30.4 (13.6)	37.6 (21.1)
R1, wR2 [%]	3.17, 8.16	3.08; 8.18
Distance N – C [Å]	1.324(2)	1.323(2)



Typical diffraction pattern ($P2_1$,
 $a = 8.3628(6)$ Å, $b = 7.0469(5)$ Å,
 $c = 15.9737(11)$ Å, $\beta = 92.210(1)^\circ$, $Z = 2$)

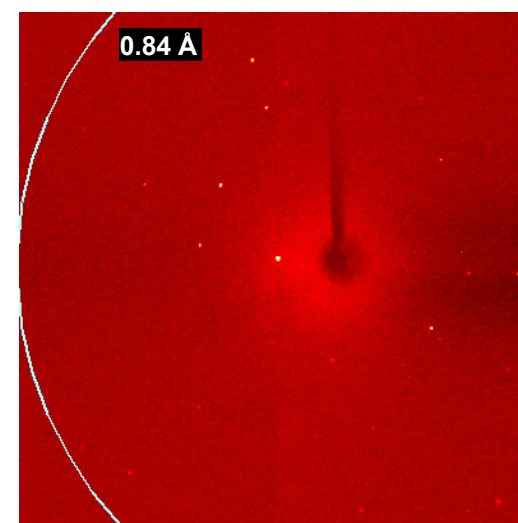
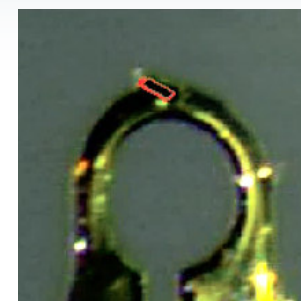


How small?



- Data from a Tiny Crystal of MOF Compound

Size [mm ³]	0.002 x 0.010 x 0.018
Source	Mo- μ S HB
Power [W]	50
Exposure time	240 s/°, 22 h
Resolution [Å]	0.83 (0.93 – 0.83)
Multiplicity	3.9 (2.2)
$\langle I/\sigma \rangle$	15.1 (4.2)
$R1, wR2$ [%]	4.27; 8.83



Typical diffraction pattern ($P2_1/m$,
 $a = 8.9215(10)$ Å, $b = 21.209(2)$ Å,
 $c = 9.1052(10)$ Å, $\beta = 107.923(3)^\circ$, $Z = 2$)

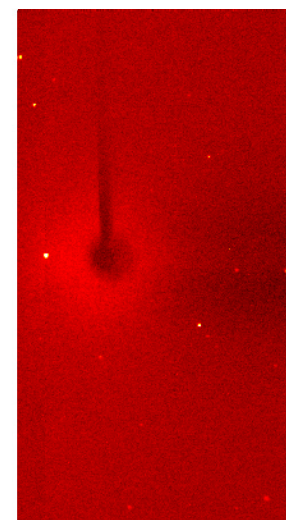
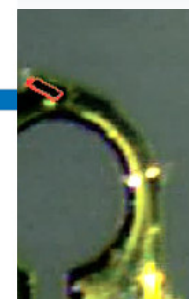
How small?



- Data from a Tir



Size [mm ³]
Source
Power [W]
Exposure time
Resolution [Å]
Multiplicity
$\langle I/\sigma \rangle$
R1, wR2 [%]



Application Note SC-XRD 502

Structural Determination of a Two Micron-sized MOF Crystal

Metal-Organic Frameworks (MOFs) are structures of great industrial and academic interest as they can be at the genesis of a series of new materials with highly attractive properties. Nowadays MOFs can be prepared very fast, under mild conditions in high yields while still combining several functions, taking advantage of the metallic centers, the organic ligands and the framework itself. Some MOFs can even outperform known materials in common industrial applications. [La(H₂bmt)(H₂bmt)(H₂O)₂·3H₂O (**1**) has outstanding catalytic activity for the methanolysis of styrene oxide in comparison to that of related MOF-type heterogeneous catalysts. In addition, the inclusion of small amounts of other lanthanides can produce highly photoluminescent materials.¹¹ **1** can be quickly prepared in 5 minutes at 330 K using microwave-assisted synthesis from the tridentate (benzene-1,3,5-triyltris(methylene)triphosphonic acid (H₂bmt) and LaCl₃·7H₂O. Nevertheless, to fully understand

microscope. The D8 VENTURE consists of a KAPPA goniometer and PHOTON 100 CMOS APS detector, equipped with a 1μS microfocus X-ray source providing Mo-Kα radiation (λ = 0.71073 Å). During the entire experiment the sample was kept at 100 K using a KRYOFLEX II low temperature device, controlled with the APEX2 software package.

The experiment

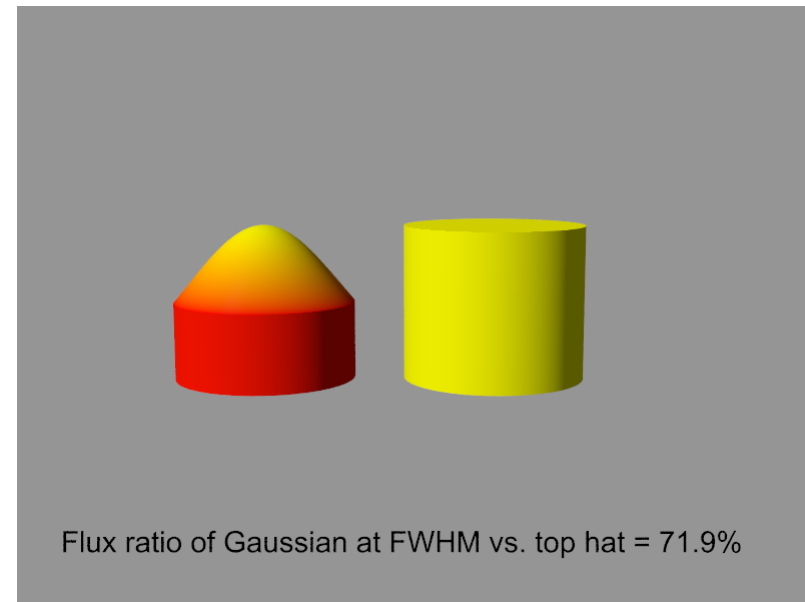
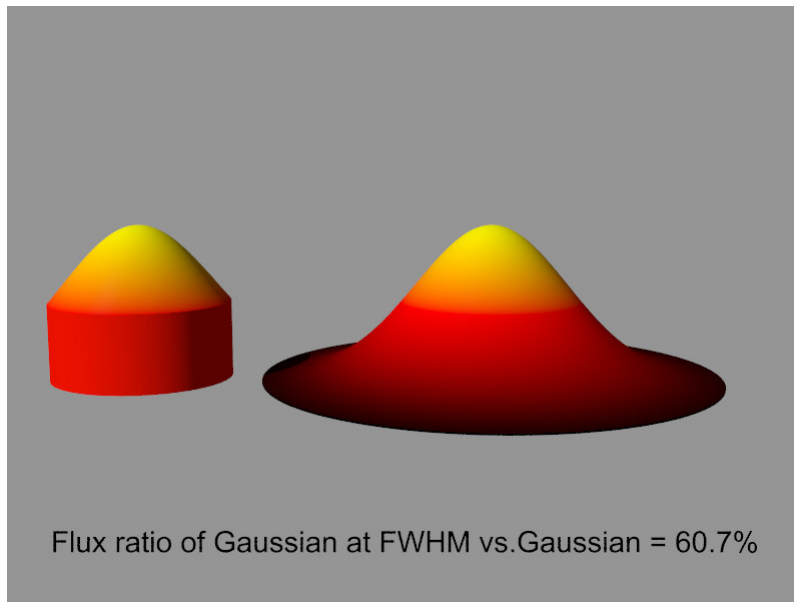
Based on a number of initial scans the unit cell determination routine of the software suite indicated a monoclinic unit cell. From the same scans 0.5 degree frames were suggested by the data collection strategy optimizer and the refined data collection strategy consisted of only three scans. Due to the weak diffraction of this very tiny crystal, an appropriate frame exposure time of 120 s was selected. A total of 645 frames were collected within just 21.5 hours.

n pattern ($P2_1/m$,
 $a, b = 21.209(2) \text{ \AA}$,
 $\alpha, \beta = 107.923(3)^\circ$, $Z = 2$)

Microfocus Source Gaussian Beam Profile

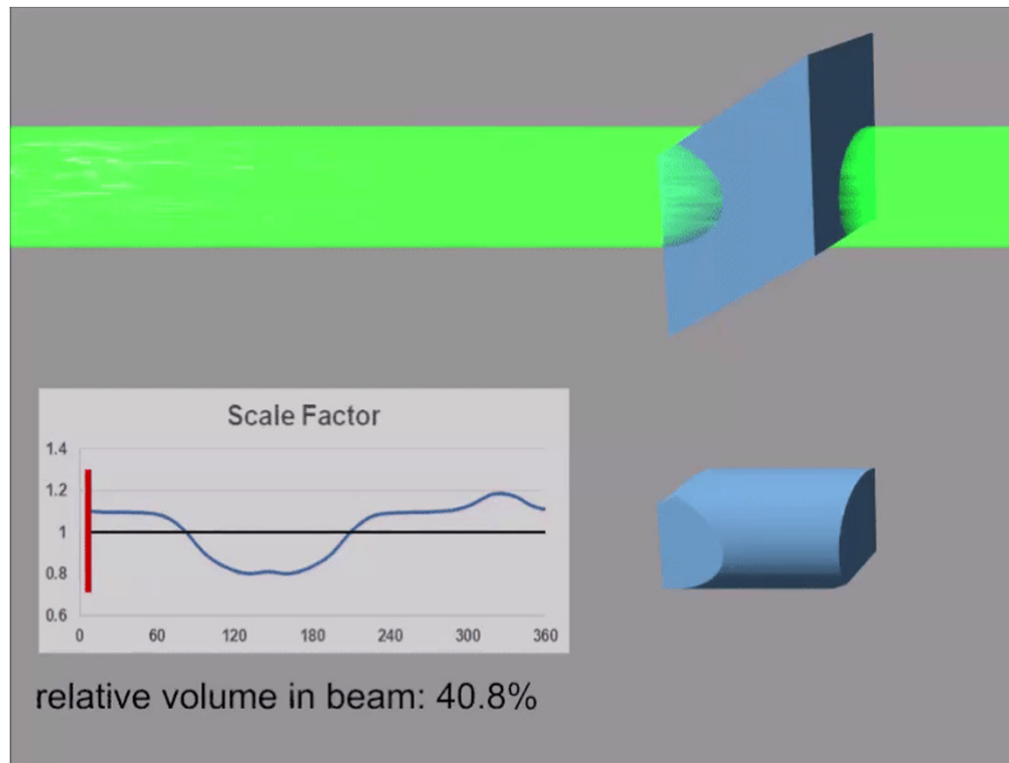


- Classic normal fine focus sources with graphite monochromators exhibit a top hat shaped beam profile
 - Flat graphite crystal
 - TRIUMPH curved graphite crystal



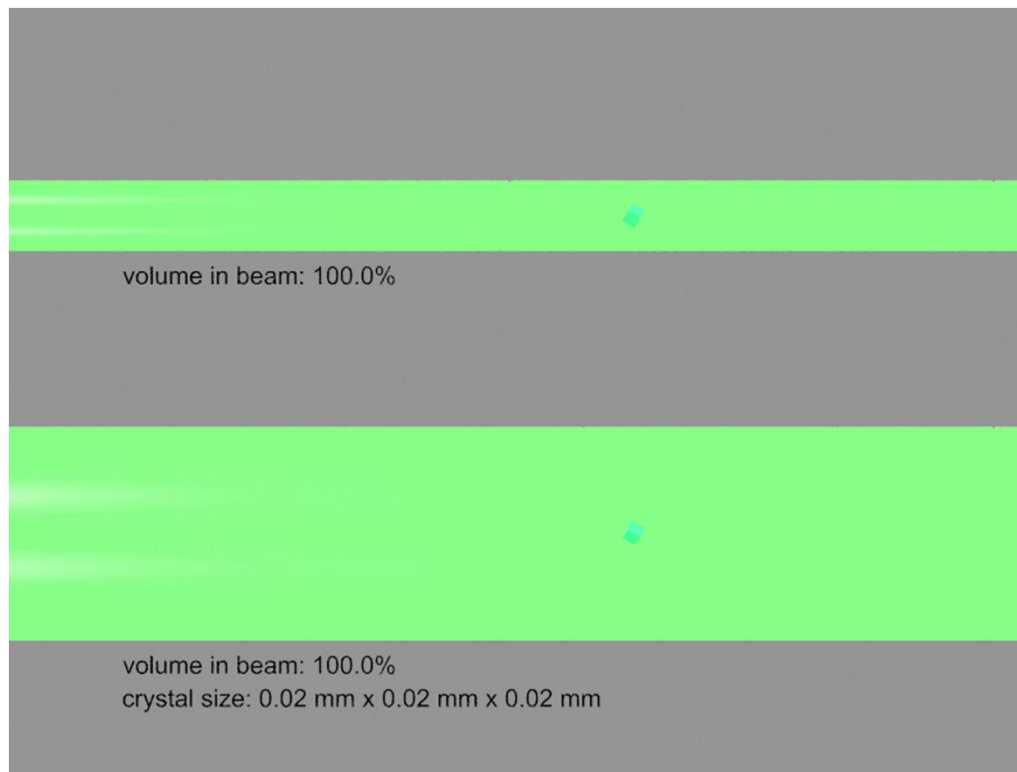
Large Crystal in Large Beam

- Rhombohedral crystal $0.2 \times 0.2 \times 0.2 \text{ mm}^3$
- Average crystal volume in beam is about 45 %
- Incident beam scale factors from 0.8 to 1.2



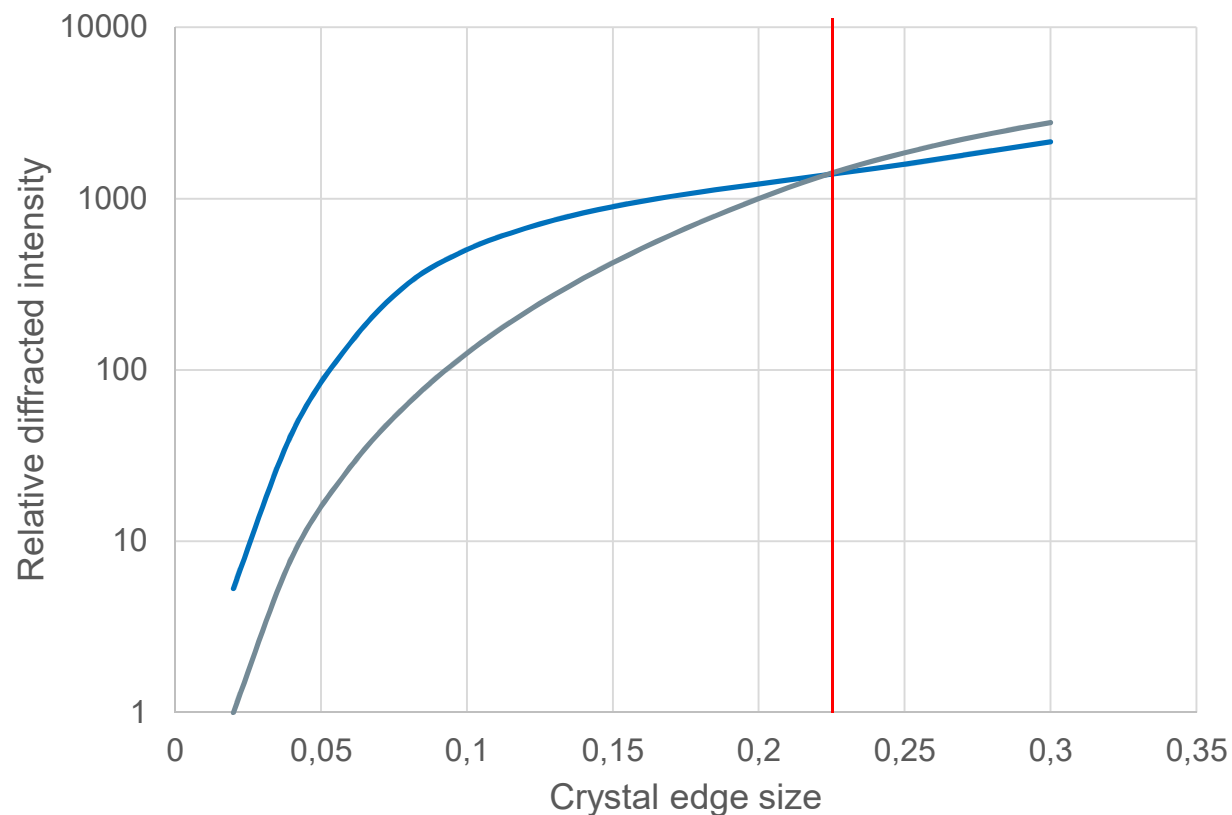
Small Beam vs. Large Beam

- Relative crystal volume in a small beam (0.1 mm) and a large beam (0.3 mm)
- The crystal is a cube in this simulation



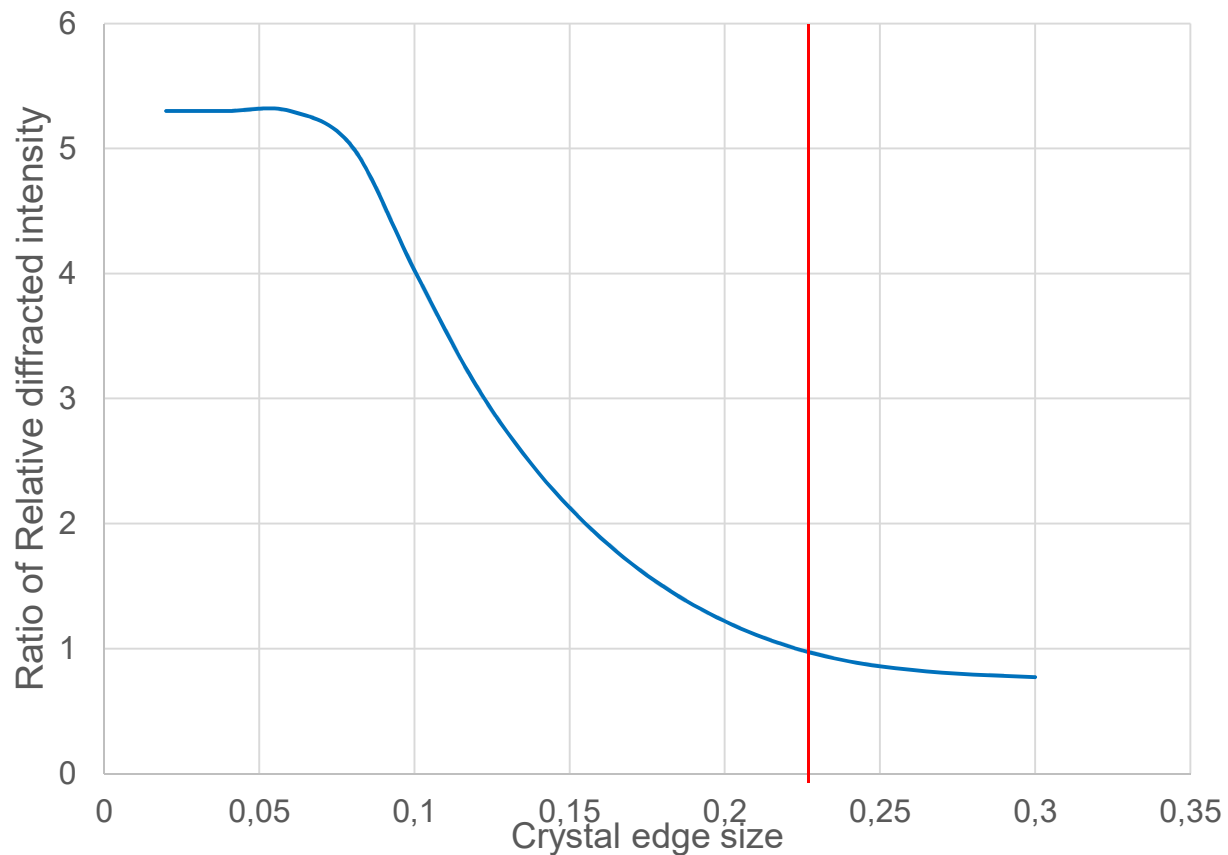
Small Beam vs. Large Beam Mo

- The small beam has a 5.3 times higher intensity (Mo)
- Relative diffracted intensity of a small beam (blue) vs large beam (gray)



Small Beam vs. Large Beam Mo

- Ratio of relative diffracted intensity from the small and the large beam

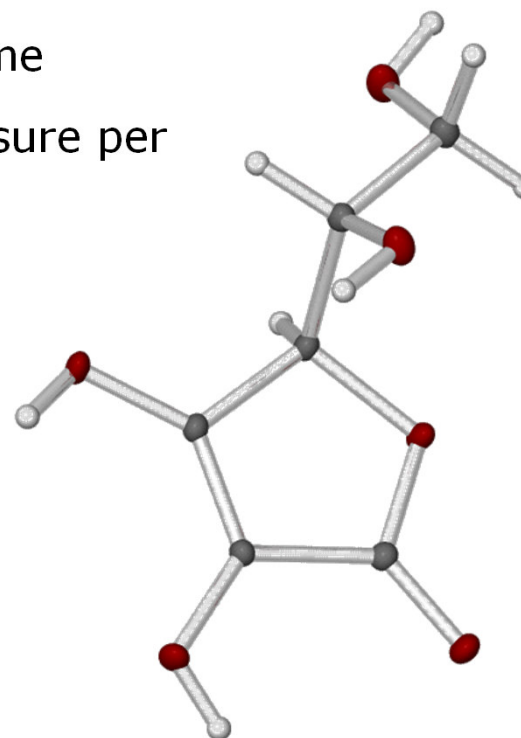


Small Crystal vs. Large Crystal

- 4 data sets were collected on Ascorbic Acid crystals
- Data were collected on a small crystal and a large crystal each with a 180 μm and a 360 μm beam
- The large crystal had a 55 times larger volume
- Data were collected to 0.65 \AA , with 10s exposure per 0.36° frame

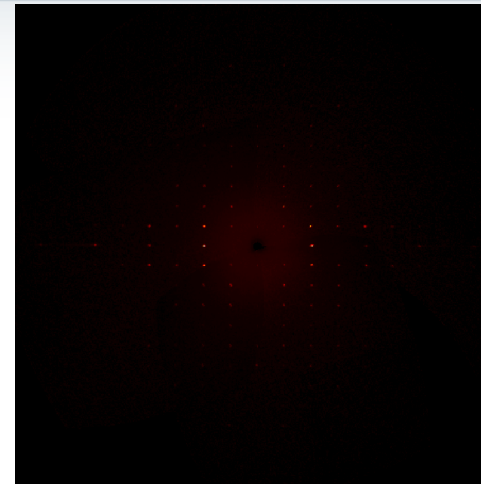
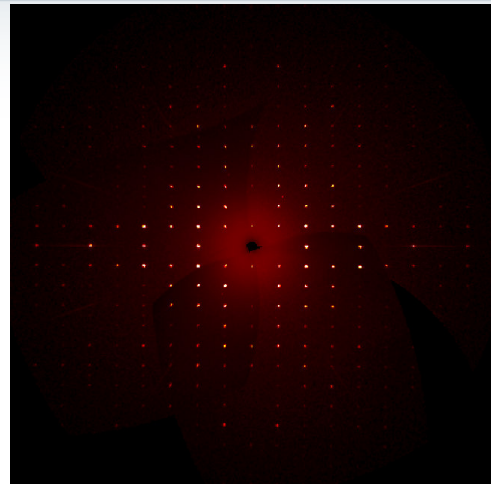
- 0.025 x 0.100 x 0.110 mm³

- 0.12 x 0.32 x 0.40 mm³



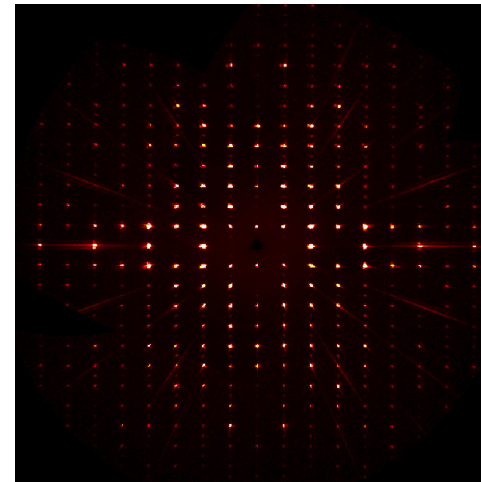
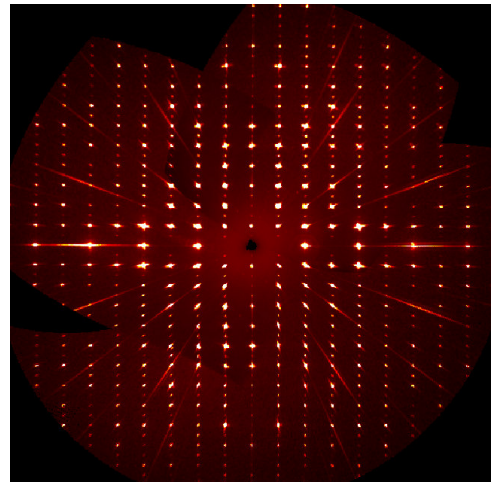
Small Crystal vs. Large Crystal

- Small crystal
small beam
- $R1 = 4.19\%$ for
3915 reflections



- Small crystal
large beam
- $R1 = 7.87\%$ for
2061 reflections

- Large crystal
small beam
- $R1 = 3.08\%$ for
4588 reflections



- Large crystal
large beam
- $R1 = 3.47\%$ for
4462 reflections

Microfocus Source Examples

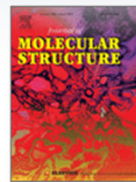


App Lab Madison – Christian Jelsch, Nancy Aceclofenac Charge Density Study



Journal of Molecular Structure

Volume 1205, 5 April 2020, 127600



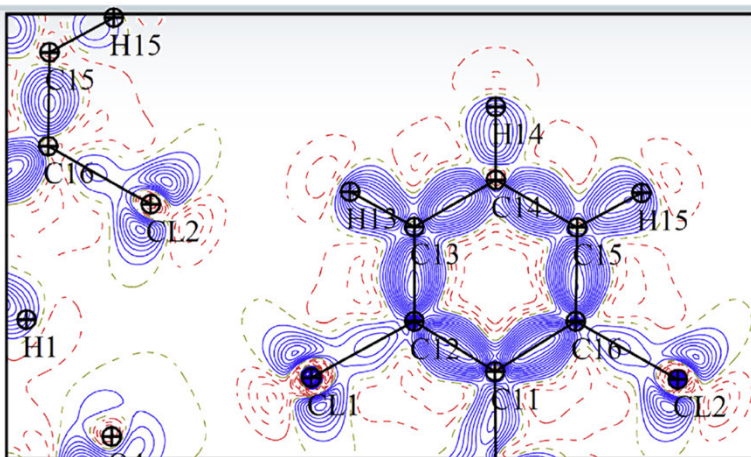
Aceclofenac and interactions analysis in the crystal and COX protein active site

Christian Jelsch ^a ✉, Rajendran Niranjana Devi ^{b, c}, Bruce C. Noll ^d, Benoît Guillot ^a, Israel Samuel ^b, Emmanuel Aubert ^a

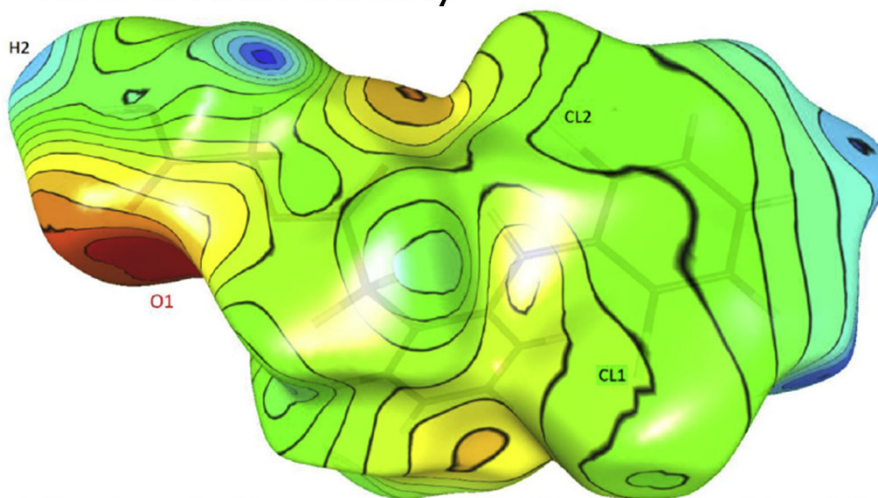
- Data from the D8 QUEST with TRIUMPH were merged with data from a D8 VENTURE for a multi-site charge density experiment
- Both crystals were larger than the beam
 - D8 VENTURE $0.108 \times 0.198 \times 0.208 \text{ mm}^3$
 - D8 QUEST $0.148 \times 0.360 \times 0.379 \text{ mm}^3$

App Lab Madison – Christian Jelsch, Nancy

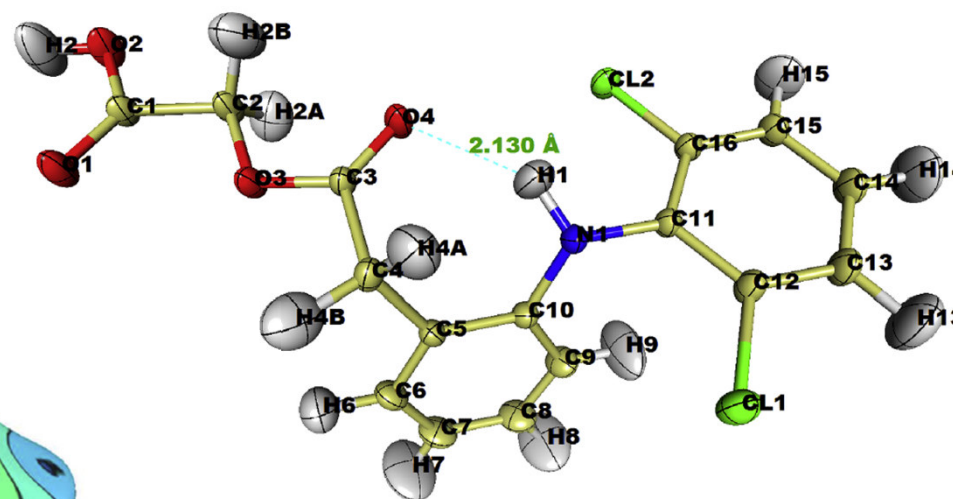
Aceclofenac Charge Density Study



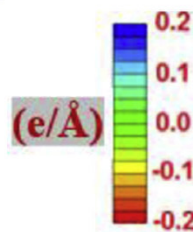
Deformation density



Electrostatic potential $V_{int}(r)$ on the Hirshfeld surface



Structure of Aceclofenac



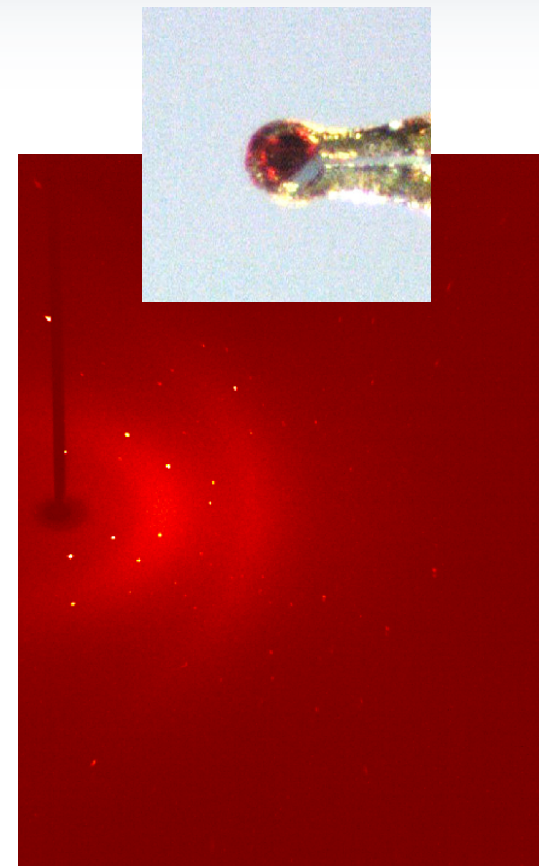
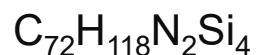
Saarland University – Scheschkewitz Lab

All-Silicon Cyclobutan-1,3-diyl as Reaction Intermediate



Data from a Small Crystal of a Stabilized
Tetrasilacyclobutan-1,3-diyl

Size [mm³]	0.02 x 0.08 x 0.08
Source	Cu-IμS 3.0 MX
Exposure time	20 s/0.5°
Resolution [Å]	0.80 (0.90 – 0.80)
Multiplicity	6.2 (4.5)
$\langle I/\sigma \rangle$	9.5 (4.7)
<i>R</i> 1, <i>wR</i> 2 [%]	5.74, 13.39



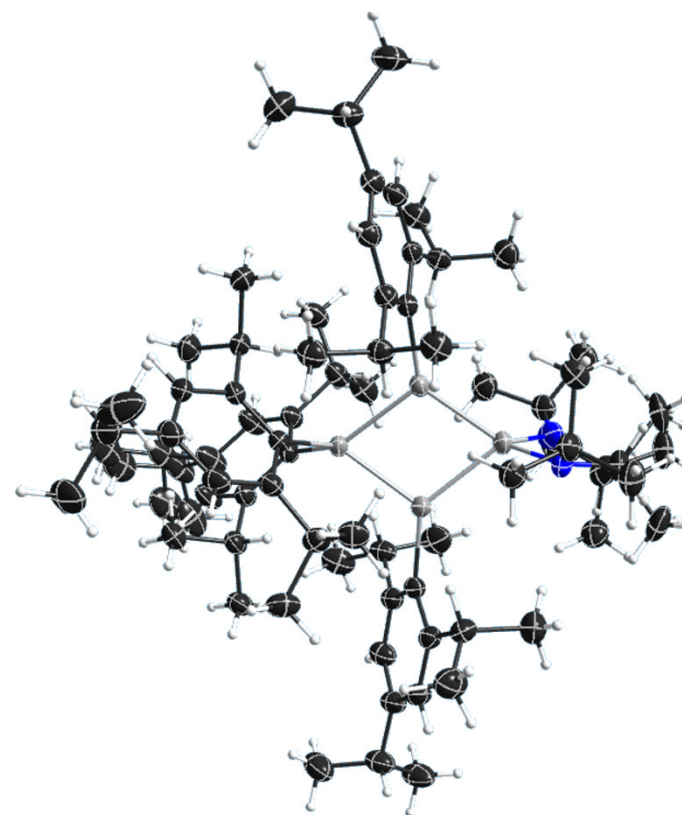
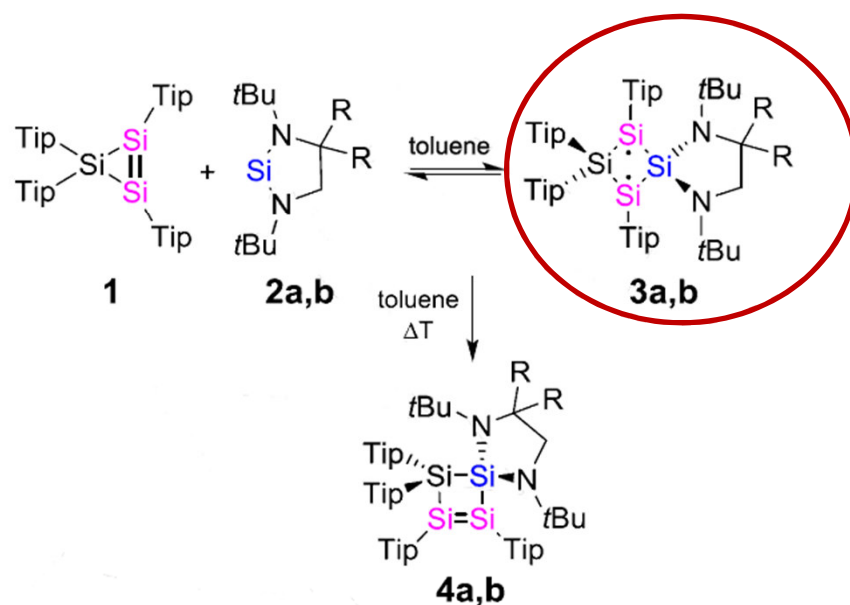
Typical diffraction pattern ($P2_1/n$,
 $a = 14.7011(4) \text{ \AA}$, $b = 22.3445(7) \text{ \AA}$,
 $c = 21.1554(7) \text{ \AA}$, $\beta = 96.007(2)^\circ$, $Z = 4$)

Saarland University – Scheschkewitz Lab

All-Silicon 1,3-Cyclobutandiyl as Reaction Intermediate



Reaction Scheme for the Formation of the Stabilized Tetrasilacyclobutan-1,3-diyl



- Encapsulated Nanodroplet Crystallization as a new robot-assisted high-throughput nanoscale crystallization method:
 - Crystals from challenging “uncrystallisable” small molecule compounds
 - Powerful tool for efficient polymorph screening

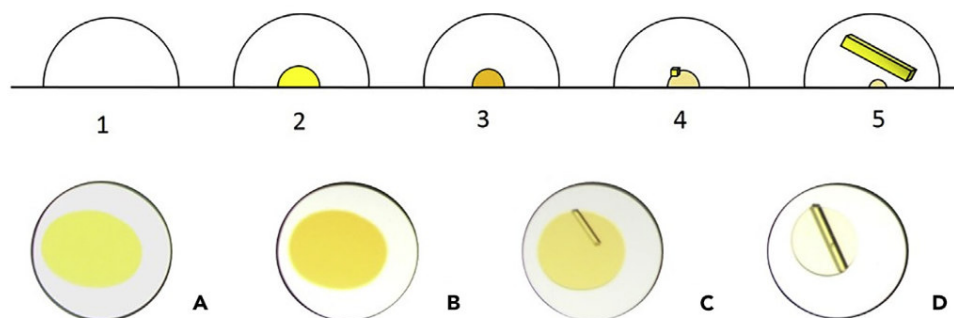


Figure 1. Cross-Section Schematic of an ENaCt Experiment (Top) and ENaCt Experiment with 200 nL Mineral Oil and 50 mg/mL ROY in DMSO (Bottom).

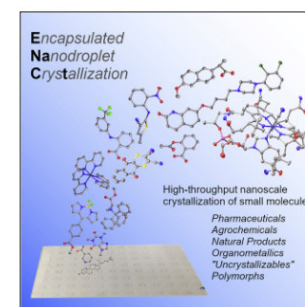
(1) Viscous inert oil dispensed onto a well of a 96-well glass plate, (2) solution of analyte in organic solvent injected into an oil droplet, (3) evaporative solvent loss to supersaturation, (4) nucleation, and (5) crystal growth. (A) solution of solvated analyte under oil, (B) evaporative solvent loss to supersaturation, (C) onset of crystal growth, and (D) complete crystallization.

Chem

CellPress

Article

Encapsulated Nanodroplet Crystallization of Organic-Soluble Small Molecules



Andrew R. Tyler, Ronnie Ragbarsingh, Charles J. McMonagle, ..., Paul Thaw, Michael J. Hall, Michael R. Probert

michael.hall@ncl.ac.uk (M.J.H.)
michael.probert@ncl.ac.uk (M.R.P.)

HIGHLIGHTS

Single crystals of small molecules are grown from nanoscale droplets of organic solvent

Discovery of the 13th polymorph (RTB) of oleanagine precursor ROY

X-ray diffraction analysis of “uncrystallizable” agrochemical dithionon

The routine crystallization of small molecules for single-crystal X-ray analysis remains a considerable experimental challenge. We report a general method for the high-throughput nanoscale crystallization of organic-soluble small molecules: encapsulated nanodroplet crystallization (ENaCt). ENaCt provides crystals suitable for X-ray analysis, allowing structural and *de novo* absolute stereochemical assignment for a diverse and challenging range of small molecules (bioactives, natural products, organometallics, etc.), as well as acting as a tool for new polymorph discovery.



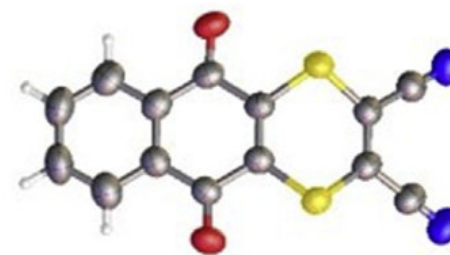
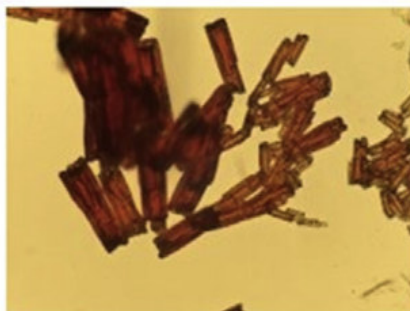
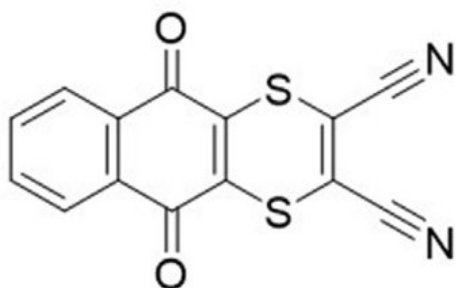
Tyler et al., Chem 6, 1–11
July 9, 2020 © 2020 The Authors. Published by
Elsevier Inc.
<https://doi.org/10.1016/j.chem.2020.04.009>

Newcastle University – Michael Probert's Lab

Crystallising the “uncrystallisable”



- First single crystal structure of an “uncrystallisable” molecule:
Case study on the fungicide Dithianon
 - Several batches showed crystals formed by Encapsulated Nanodroplet Crystallization
 - Data collected with D8 VENTURE with Cu- μ S 3.0 (0.05 x 0.11 x 0.21 mm³)



Dithianon (7): $R_1 = 0.048$, $wR_2 = 0.1262$, Residual e^- density ($e^- \text{Å}^3$) min = -0.2 and max = 0.4

200 nL PDMSO, 50 nL of 12.5 mg/mL of dithianon in DMF, 25 nL 2-methyl-2,4-pentanediol.

MIT – Peter Mueller’s Lab (I μ S 3.0 MX) Nucleoside Polyphosphates as RNase inhibitors



J|A|C|S
JOURNAL OF THE AMERICAN CHEMICAL SOCIETY

Cite This: *J. Am. Chem. Soc.* 2019, 141, 18400–18404

Communication

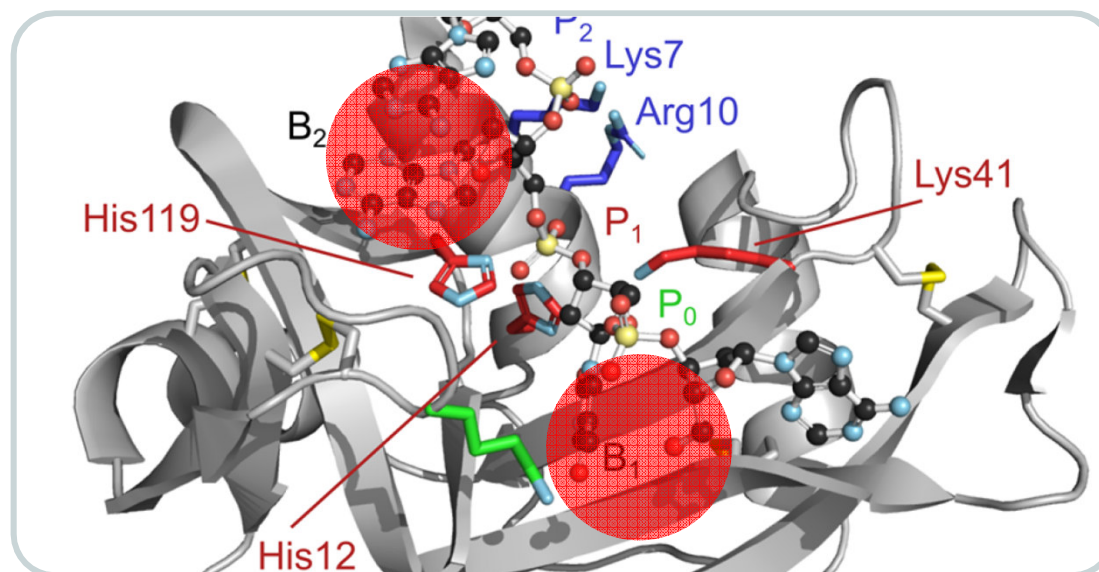
pubs.acs.org/JACS

Nucleoside Tetra- and Pentaphosphates Prepared Using a Tetraphosphorylation Reagent Are Potent Inhibitors of Ribonuclease A

Scott M. Shepard,[†] Ian W. Windsor,[†] Ronald T. Raines,^{*†} and Christopher C. Cummins^{*†}

Department of Chemistry, Massachusetts Institute of Technology, Cambridge Massachusetts 02139, United States

- RNase active sites B1 and B2 bind Uridine and Adenosine Nucleoside Polyphosphates

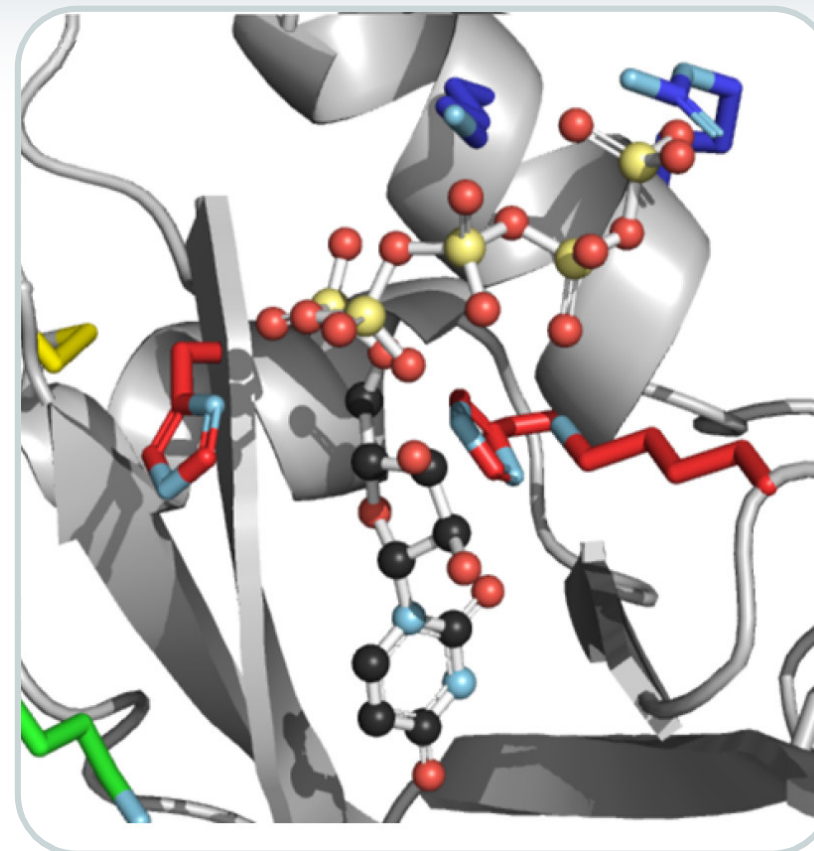
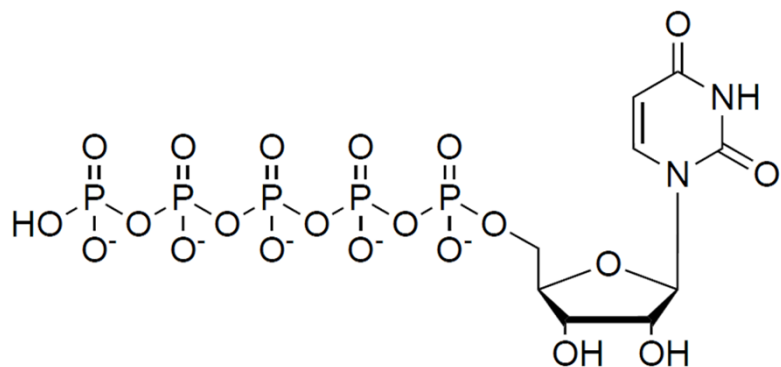


MIT – Peter Mueller’s Lab (I μ S 3.0 MX)

Nucleoside Polyphosphates as RNase inhibitors



- RNase A ligand structures were solved by molecular replacement using the Phaser program as implemented in PHENIX.
- Refinement was performed with phenix.refine, and model building was conducted with COOT.
- Restraints for inhibitors were prepared with eLBOW in PHENIX and placed with COOT



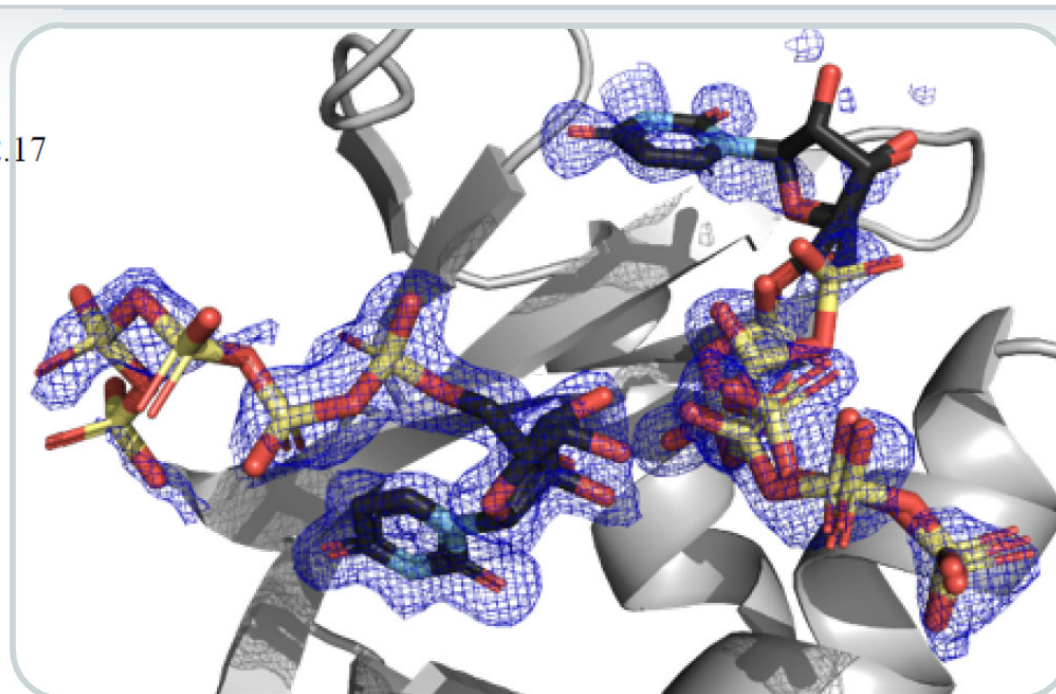
p₅U only binds in the B1 site and alternatively targets the P₁ and P₂ subsites

MIT – Peter Mueller’s Lab (I μ S 3.0 MX)

Nucleoside Polyphosphates as RNase inhibitors



Ligand (PDB ID)	psU (6pvx)
Data collection	
Space group	C121
<i>a</i> , <i>b</i> , <i>c</i> (Å)	100.54, 32.64, 72.17
α , β , γ (°)	90, 90.4, 90
Wavelength (Å)	1.54178
Resolution (Å)	29.42–1.55 (1.61–1.55)
Total Reflections	413831 (21558)
Unique Reflections	34001 (2948)
Multiplicity	12.1 (7.3)
Completeness (%)	98.7 (87.1)
Mean <i>I</i> / σ (<i>I</i>)	25.4 (3.0)
Wilson <i>B</i> factor (Å ²)	14.68
<i>R</i> _{merge}	0.060 (0.552)
<i>R</i> _{meas}	0.062 (0.594)
<i>R</i> _{p.i.m.}	0.017 (0.215)
CC _{1/2}	1.000 (0.823)
Refinement	
Reflections	
Work set	33999 (2948)
Test set	1983 (176)
<i>R</i> _{work}	0.1991 (0.2557)
<i>R</i> _{free}	0.2282 (0.2939)
R.m.s.d., bond lengths (Å)	0.006
R.m.s.d., bond angles (Å)	0.85



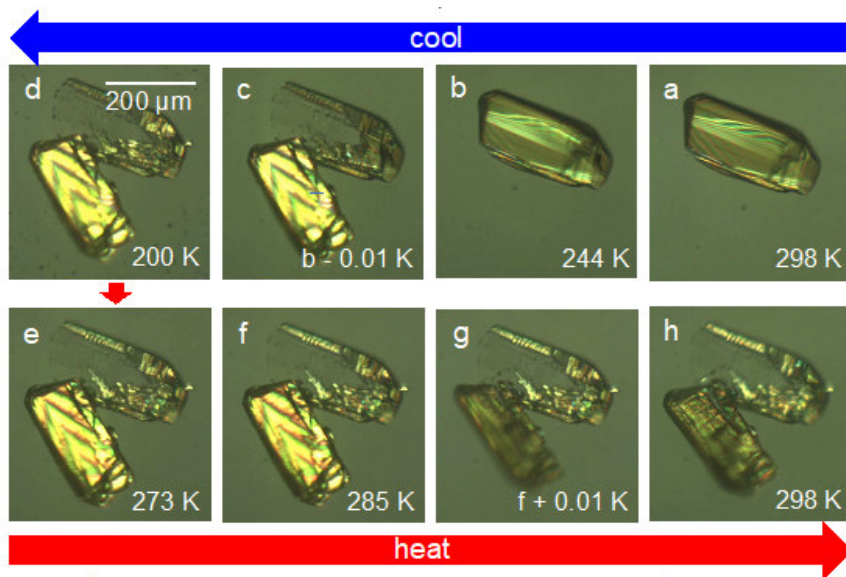
Densities of ligands bound to RNase A.
2Fo - Fc maps at 1 σ

UW Madison – Ilia Guzei's Lab (I μ S 3.0 EF) Light sensitive RT polymorph of nifedipine – RT structure

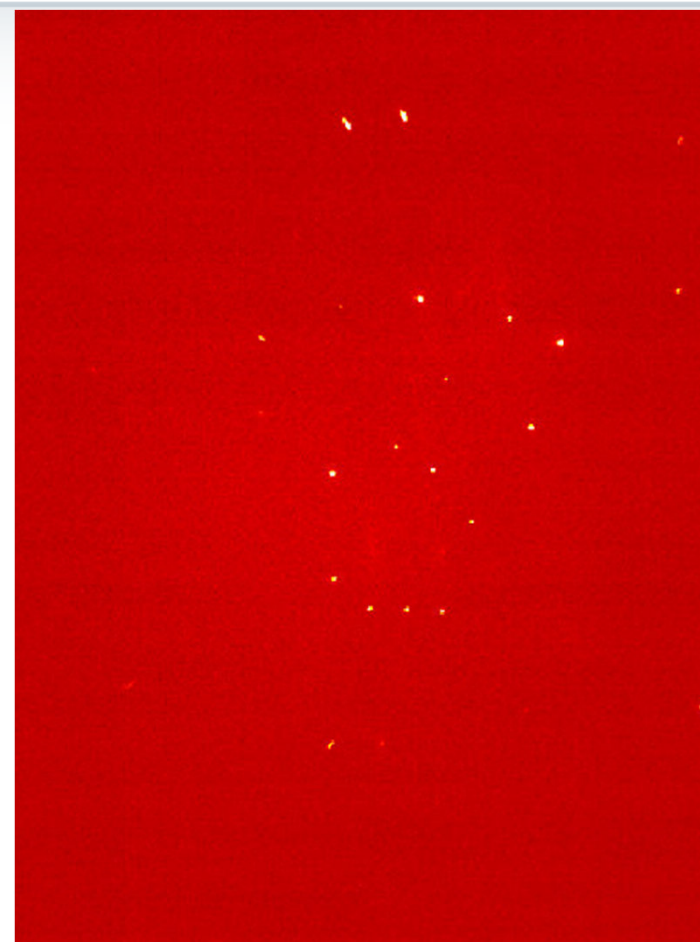


Submitted for publication:
Reversible solid-state transformations:
A new mechanism based on nitro
torsion illustrated by nifedipine
polymorphs.

Yue Gui, Xin Yao, Ilia A. Guzei, Michael M.
Aristov, Junguang Yu, Lian Yu



Solid-state transformations of the γ polymorph



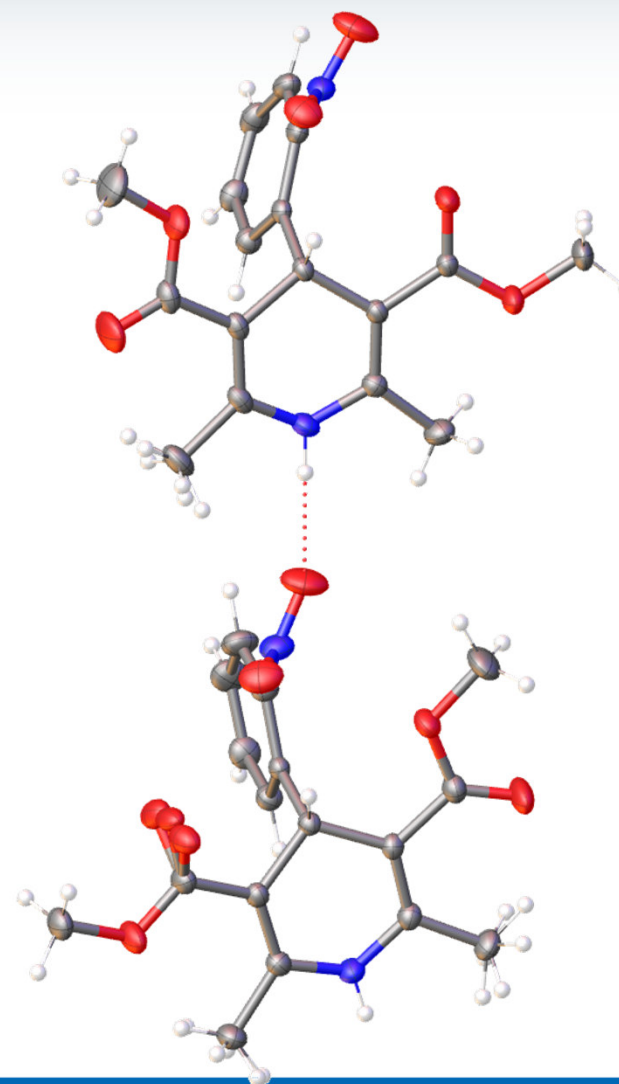
Diffraction pattern of a
 $0.04 \times 0.04 \times 0.04 \text{ mm}^3$ crystal

UW Madison – Ilia Guzei's Lab (I μ S 3.0 EF)

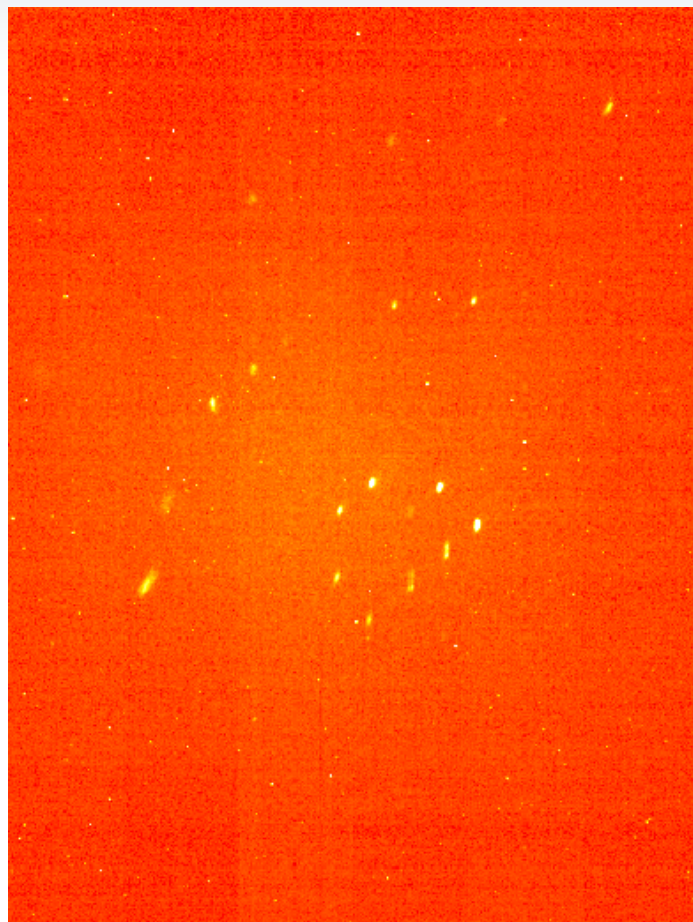
Light sensitive RT polymorph of nifedipine – RT structure



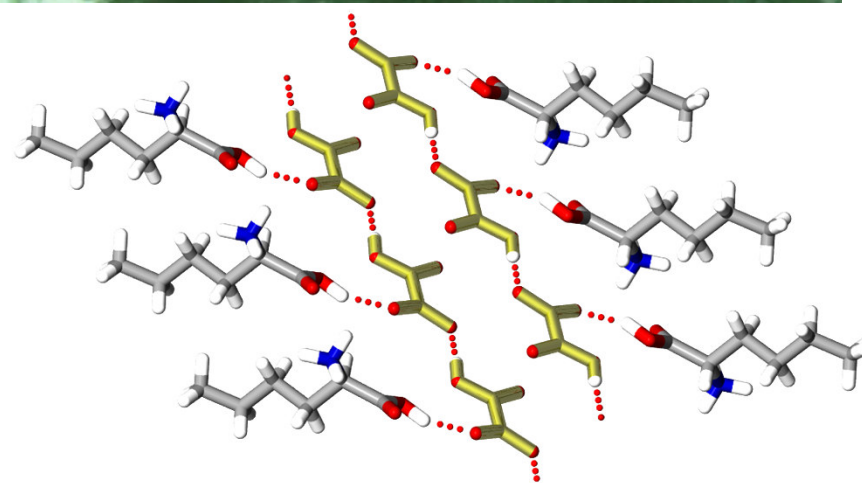
Form	γ'
T, K	296
a, Å	11.450
b, Å	12.301
c, Å	12.356
α , deg	75.63
β , deg	89.09
γ , deg	84.93
V, Å ³	1679.19
space group	P $\bar{1}$
R1, %	4.38



Whitworth University – Kraig Wheeler's Lab
(I μ S 3.0 EF)
Racemic Norleucinium Oxalate



Diffraction pattern of a
 $0.028 \times 0.122 \times 0.401 \text{ mm}^3$ crystal

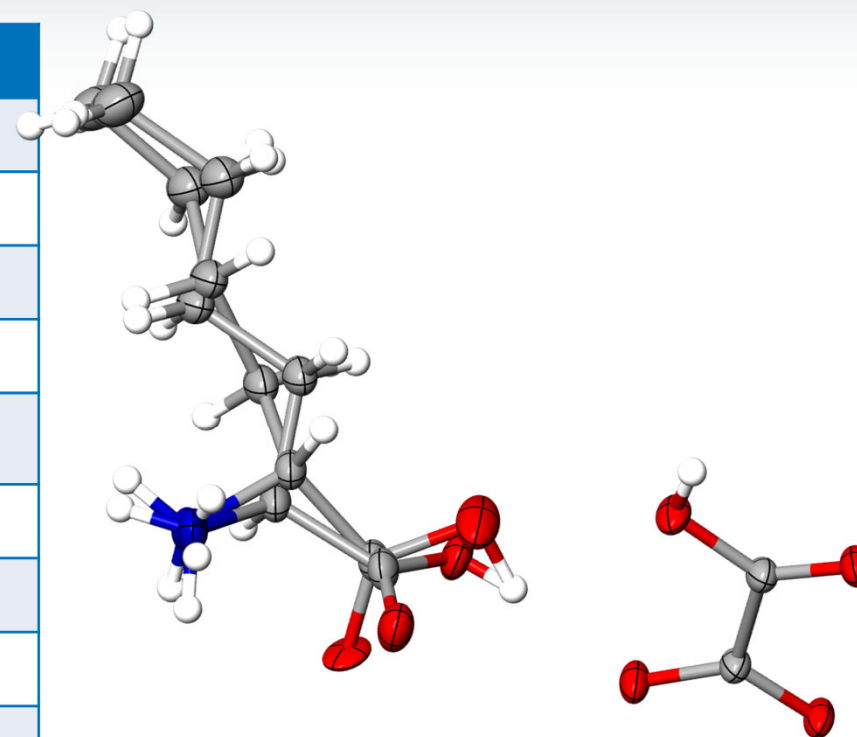


Whitworth University – Kraig Wheeler’s Lab
(I μ S 3.0 EF)

Racemic Norleucinium Oxalate

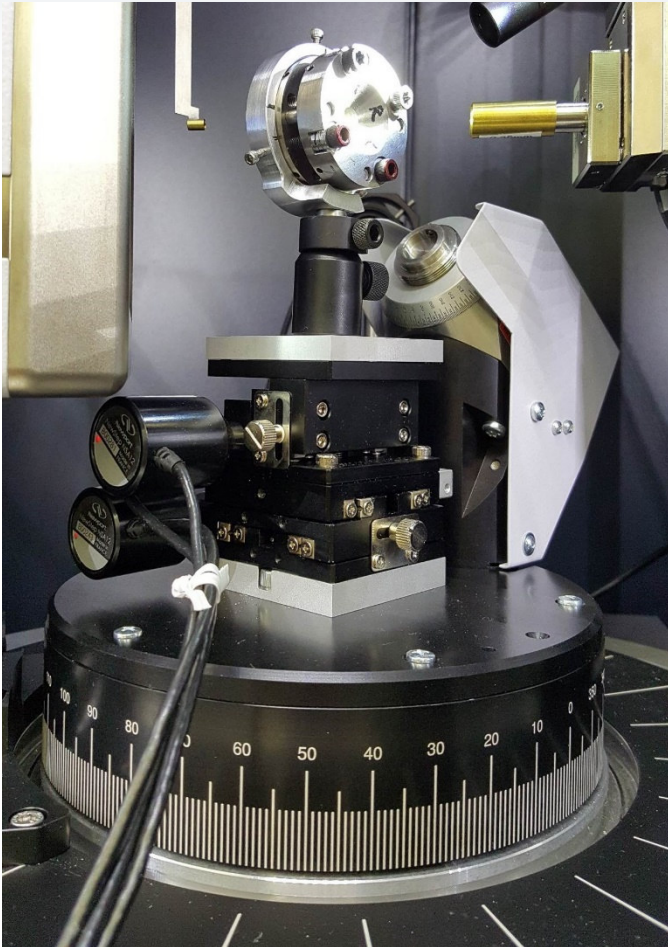


Norleucinium Oxalate	
T, K	100
a, Å	5.6270(5)
b, Å	9.4327(9)
c, Å	10.4431(10)
α, deg	88.922(4)
β, deg	75.976(4)
γ, deg	83.757(4)
v, Å³	534.57(9)
space group	P $\bar{1}$
R1, %	4.76



Norleucinium 90:10 disorder

UH Manoa - Przemyslaw Dera ($I\mu\text{S}$ 3.0 Ag) High pressure setup with 50 μm beam



Motorized heavy-duty (10lb load capacity) XYZ sample stage is small enough that motors fit underneath the detector. The motorized stage can accommodate cooling sample holder (not shown in the picture) for resistive heating experiments as well as open cradle chi stage.

UH Manoa - Przemyslaw Dera (I μ S 3.0 Ag)

High pressure setup with 50 μ m beam



	D8 VENTURE UHM	PX ² , MAR165 CCD/APS	D8 VENTURE UHM
Pressure	ambient	2 GPa	2 GPa
Wavelength	0.56086 Å	0.43000 Å	0.56086 Å
Crystal system	Monoclinic		
Space group	C2/c		
Unit cell dimensions	a = 9.835(7) Å b = 18.01(2) Å c = 5.303(2) Å b = 104.71(4)°	a = 9.8360(15) Å b = 18.068(11) Å c = 5.2730(7) Å b = 104.801(13)°	a = 9.814(2) Å b = 18.076(4) Å c = 5.284(2) Å b = 104.78(3)°
Volume	908.6(13) Å ³	906.0(6) Å ³	906.4(4) Å ³
Theta range for data collection	3.17 to 27.96°	1.46 to 20.20°	1.91 to 18.13°
Exposure time	20 sec/deg	10 sec/deg	40 sec/deg
Index ranges	-16<=h<=16, -29<=k<=30, -8<=l<=7	-11<=h<=12, -12<=k<=8, -5<=l<=7	-8<=h<=8, -17<=k<=17, -5<=l<=5
Reflections collected	5959	1045	3765
Independent reflections	2254 [R(int) = 0.0409]	375 [R(int) = 0.0740]	364 [R(int) = 0.1003]
Completeness to	27.96° / 98.5 %	20.20° / 18.5 %	18.13° / 54.2 %
Data / restraints / parameters	2254 / 0 / 104	375 / 0 / 63	364 / 0 / 51
Goodness-of-fit on F ₂	1.043	1.035	1.006
Final R indices [I > 2 σ (I)]	R1 = 0.0341, wR2 = 0.0718	R1 = 0.0437, wR2 = 0.1187	R1 = 0.0728, wR2 = 0.1731
R indices (all data)	R1 = 0.0500, wR2 = 0.0820	R1 = 0.0438, wR2 = 0.1187	R1 = 0.1203, wR2 = 0.2129
Largest diff. peak and hole	0.799 and -0.692 e.Å ⁻³	0.492 and -0.430 e.Å ⁻³	0.735 and -0.662 e.Å ⁻³

Comparison single crystal data collected on X-ray Atlas at ambient and high pressure, and at APS experimental station 13BM-C on the same sample of ferroactinolite Ca₂(Mg_{2.5-5.0}Fe²⁺_{2.5-5.0})Si₈O₂₂(OH)₂ amphibole. The sample crystal was 20 × 20 × 5 micrometers in size, loaded in Ne.

IU Bloomington- Maren Pink's Lab (I μ S 3.0 Mo, I μ S DIAMOND Cu) Natural Products - Ladderanes



Angewandte
International Edition
Chemie

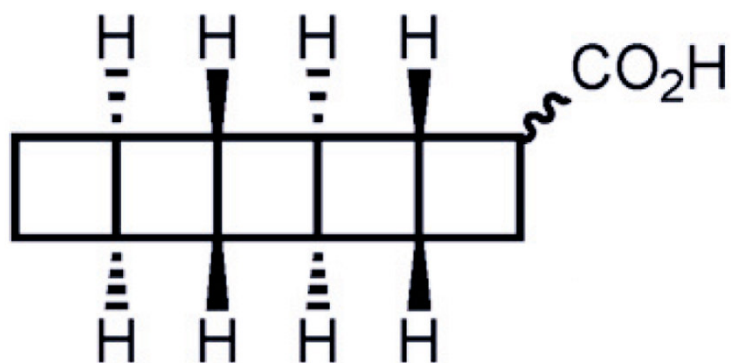


A Journal of the
German
Chemical Society

Research Article | Free Access

Lessons in Strain and Stability: Enantioselective Synthesis of (+)-[5]-Ladderanoic Acid

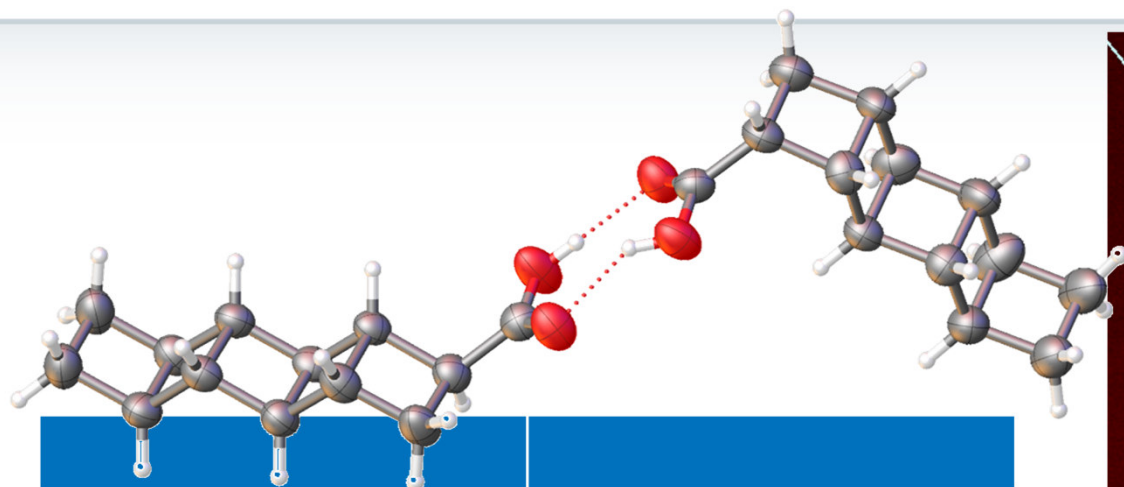
Erin N. Hancock, Erin L. Kuker, Prof. Dean J. Tantillo, Prof. M. Kevin Brown



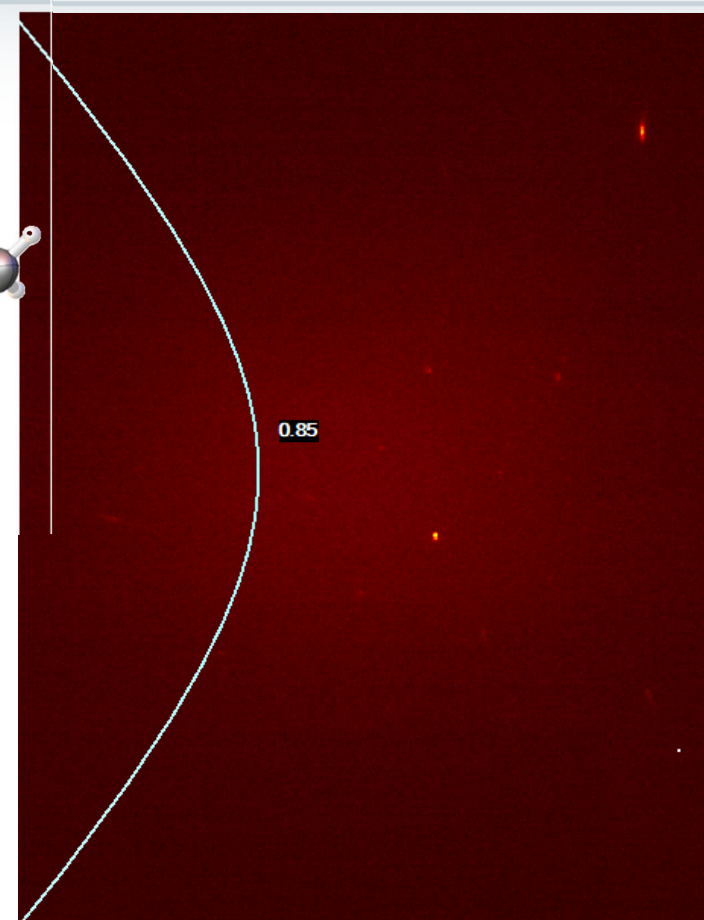
...The ladderane family of natural products is a unique class of molecules that is characterized by a series of fused cyclobutanes.^{1, 2} Because of their complex structure and **unknown biological function,**³ several groups have developed routes to these molecules (Scheme 1)...

These ladderane crystals are super thin and bendable. So, high intensity sources are a must. Without the I μ S, I would have taken them to the synchrotron. The I μ S has taken a chunk out of what we would have to bring to ChemMatCARS otherwise.

IU Bloomington- Maren Pink's Lab (I μ S DIAMOND Cu) Natural Products - Ladderanes

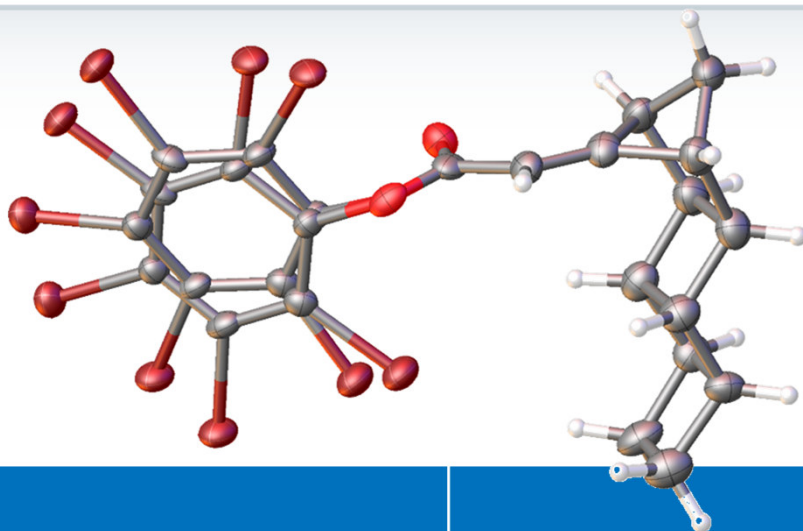


Crystal system	Monoclinic,
space group	C2
Unit cell dimensions	a = 8.9241(6) Å
	b = 6.1187(4) Å
	c = 38.303(2) Å
	$\beta = 90.524(4)^\circ$.
R1	7.59%
wR2	20.71%

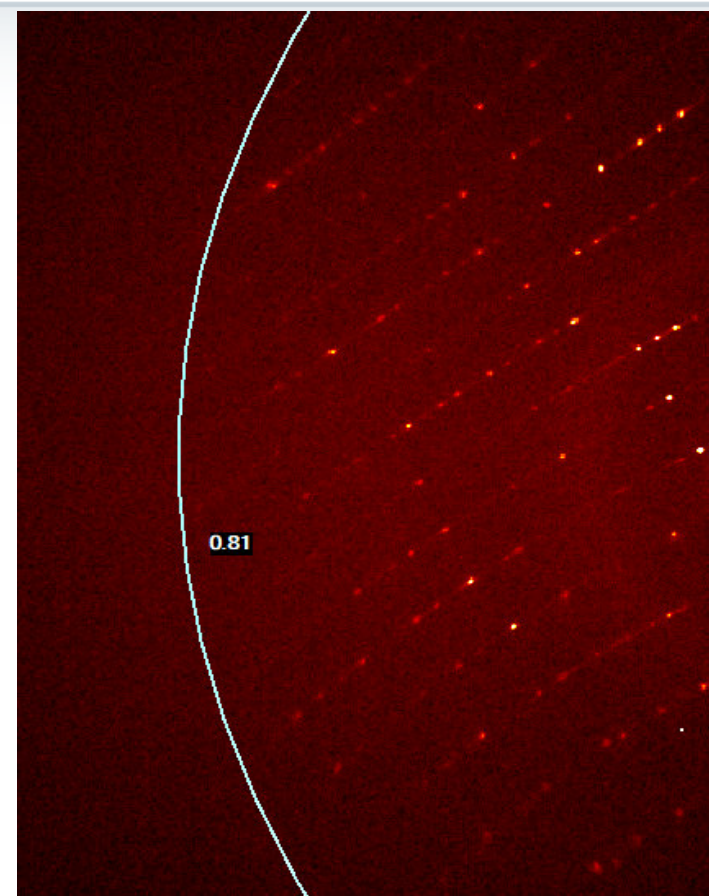


Diffraction pattern of a
 $0.09 \times 0.06 \times 0.01 \text{ mm}^3$ crystal $25\text{s}/0.5^\circ$

IU Bloomington- Maren Pink's Lab (I μ S 3.0 Mo) Natural Products - Ladderanes



Crystal system	Orthorhombic,
space group	P2 ₁ 2 ₁ 2
Unit cell dimensions	a = 25.325(3) Å
	b = 27.082(3) Å
	c = 9.0645(10) Å
R1	5.63%
wR2	12.95%



Diffraction pattern of a
0.09 × 0.07 × 0.02 mm³ crystal 20s/0.5°



Like what you learned in this webinar?

Subscribe to Bruker's ***FIRST Newsletter*** to get webinar announcements, technical articles, and X-ray crystallography news delivered right to your inbox.

Subscribe at:

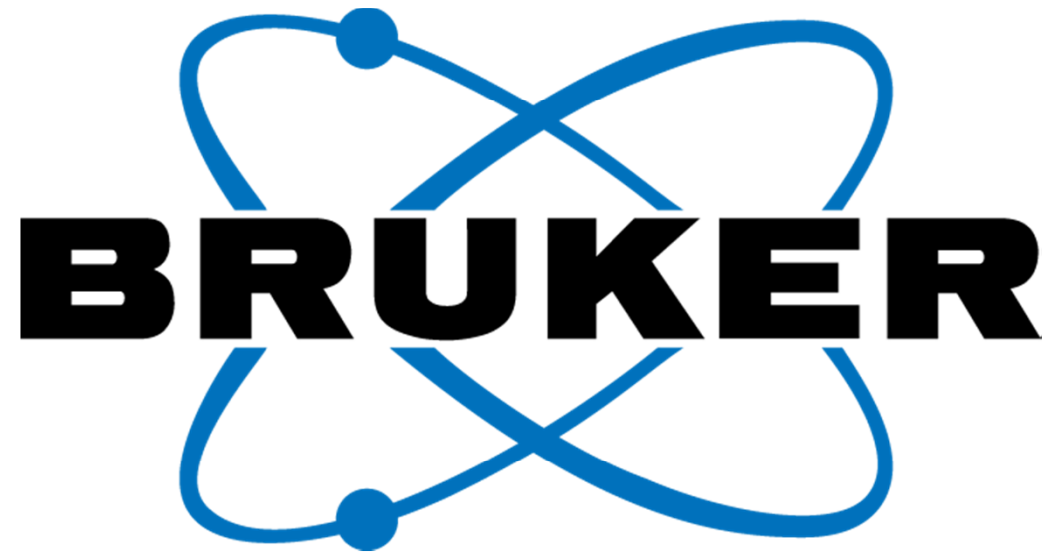
<https://www.bruker.com/news/newsletter/first-newsletter-registration.html>



Webinars – Live and On-Demand

Register for future webinars and view webinar recordings at:

<https://www.bruker.com/service/education-training/webinars/sc-xrd.html>



Innovation with Integrity